Weierstraß-Institut
für Angewandte Analysis und Stochastik

Leibniz-Institut im Forschungsverbund Berlin e. V.

Preprint ISSN 2198-5855

Optimal beam forming for laser materials processing

Manuel J. Arenas[1], Dietmar Hömberg[1,2,3], Robert Lasarzik[2]

submitted: December 22, 2023

[1] Technische Universität Berlin
Institut für Mathematik
Str. des 17. Juni 136
10623 Berlin
Germany
E-Mail: arenas@math.tu-berlin.de

[2] Weierstrass Institute
Mohrenstr. 39
10117 Berlin
Germany
E-Mail: dietmar.hoemberg@wias-berlin.de
robert.lasarzik@wias-berlin.de

[3] Department of
Mathematical Sciences
NTNU
Alfred Getz vei 1
7491 Trondheim
Norway

No. 3080
Berlin 2023

2020 *Mathematics Subject Classification.* 35A35, 35Q35, 49J20, 76A15.

Key words and phrases. Quasi-linear elliptic equation, transport dominated PDE, additive manufacturing, selective laser melting, finite element method, simulation.

The authors are grateful for the support by the European Union's Horizon 2020 research and innovation programme under the Marie Skłodowska-Curie grant agreement No. 675715 (MIMESIS).

Edited by
Weierstraß-Institut für Angewandte Analysis und Stochastik (WIAS)
Leibniz-Institut im Forschungsverbund Berlin e. V.
Mohrenstraße 39
10117 Berlin
Germany

Fax: +49 30 20372-303
E-Mail: preprint@wias-berlin.de
World Wide Web: http://www.wias-berlin.de/

Optimal beam forming for laser materials processing

Manuel J. Arenas, Dietmar Hömberg, Robert Lasarzik

Abstract

We investigate an optimal control problem related to laser material treatments such as welding, remelting, hardening, or the 3D printing of metal components. The mathematical model leads to the investigation of a quasilinear elliptic state system with additional non-monotone lower-oder terms. We analyze the state system, derive first order optimality conditions and show first results for beam shaping.

1 Introduction

The laser intensity distribution on the workpiece is one of the main parameters to optimize material treatments such as laser welding, remelting, and hardening [1]. In additive manufacturing techniques like selective laser melting (SLM) with Gaussian shaped intensity profiles, a common problem is that the powder is overheated in the center of the laser spot. An excess of the energy may even lead to material evaporations and chemical decompositions [2]. At the same time the powder does not attain the necessary processing temperature at the periphery of the spot, and the energy is essentially lost by heat diffusion in the treated body.

Modern optics proposes therefore shaping a laser beam that provides alternative laser power density distributions like a flat-top or even a bimodal intensity distribution. In recent years many contributions can be found in engineering literature studying the effect of various intensity distributions on the actual thermal process, see, e.g., [3, 4] and the references therein. However, a general strategy how to find the best energy distribution for a given laser material process so far is not available.

In the present paper we tackle this problem as a PDE-constrained optimal control problem. To this end we consider a rather generic laser beam material treatment process on a metal workpiece, which exhibits changes in its microstructure upon heating and subsequent cooling. In contrast to previous investigations, where laser power and/or velocity served as a control [5], we focus on the shape of the intensity distribution. Hence, we assume constant velocity and power and since the laser beam cross section is usually small as compared to the dimensions of the treated body for which we assume a flat surface, we consider a quasistationary setting.

From analytical point of view, the main novelty of the article at hand is that optimality conditions could be derived for this involved nonlinear elliptic system. There are already several articles treating quasi-linear systems (see for instance [6], [7], [8], and references therein). In comparison to the previous works we deal with a quasilinear elliptic equation for vector-valued functions. But the main difficulty is rather hidden in the lower order terms, since these are non-monotone, which is essentially new up to our knowledge. The non-monotone terms can be handled due to their special structure, which allows to prove a comparison principle for the considered system. This comparison principle adapts the proof in Casas and Tröltzsch [6], which originates from Křížek and Liu [9] to the considered system. We extend this technique to incorporate the non-monotone lower-order terms, which then allows to derive first order optimality conditions for the system.

The paper is organized as follows. In Section 2, we describe the laser treatment model, consisting of a quasi-stationary heat equation coupled with a set of equations which describe the phase transitions causing the assumed changes of microstructure. We analyse the system of equations in Section 3. In Section 4 we derive a linearised version of the state equations. Section 5 is devoted to establish the optimal control problem which numerical resolution approach is given in Section 6 followed by first numerical results for beam shaping to achieve a flattened heating profile.

2 Model

The goal of the model is to investigate the heat distribution in a metal plate subject to the action of a moving laser. Moreover, we asssume that this laser may cause phase transitions such as the melting and subsequent recrystallization. We assume that the big size of the metal plate in comparison to the area of influence of the laser allows to consider that a quasi-stationary state is reached in an area around the heat source denoted by Ω. Accordingly, for the temperature θ in the plate, we can employ the quasi-stationary state heat equation [10],

$$\rho C_p(\theta)(\boldsymbol{v}\cdot\nabla\theta) - \nabla\cdot(\tilde{\kappa}(\theta)\nabla\theta) + \rho\boldsymbol{L}\cdot\tilde{\boldsymbol{f}}(\theta,\boldsymbol{\zeta}) = Q. \quad \text{in } \Omega. \tag{2.1}$$

Different material parameters are required for this equation: density ρ, heat capacity $C_p(\theta)$ and thermal conductivity $\tilde{\kappa}(\theta)$. One important aspect is that these properties are temperature dependent, adding nonlinearities to equation (2.1).The velocity $\boldsymbol{v}$ is a vector which, in this case, has only x as non-zero component as the trajectory of the plate is a straight line along the x axis: $\boldsymbol{v} = (v,0,0)^T$. The term $\rho\boldsymbol{L}\cdot\tilde{\boldsymbol{f}}(\theta,\boldsymbol{\zeta})$ corresponds to the heat absorbed and released during phase transitions, known as latent heat. The heat by the phase transformations is determined by the material density ρ, the latent heat $\boldsymbol{L}$ and function $\tilde{\boldsymbol{f}}$. Each component $\boldsymbol{L}_i$ and $\tilde{\boldsymbol{f}}_i$ for $i = 1,\dots,m$ corresponds to a phase transformation. As an example, in case of steel, the model could include the liquid phase, the high temperature phase austenite and the martensite phases, see [5], then we would have

$$\boldsymbol{\zeta} = (l,a,m)^T \quad \text{and} \quad \boldsymbol{f} = (f_l(\theta,l), f_a(\theta,l,a), f_m(\theta,l,a,m))^T. \tag{2.2}$$

The right-hand side Q in (2.1) will be the heat contribution according to the laser and therewith the control variable.

As seen in (2.1), the phase transitions in steel have an effect on the temperature distribution. Accordingly we introduce a set of equations corresponding to each transformation in steel occurring during flame cutting: solid-solid changes and solid-liquid (melting). The concentration of each transformation is stored in $\boldsymbol{\zeta}$ component-wise,

$$(\boldsymbol{v}\cdot\nabla)\boldsymbol{\zeta} - \varepsilon\Delta\boldsymbol{\zeta} - \tilde{\boldsymbol{f}}(\theta,\boldsymbol{\zeta}) = 0 \quad \text{in } \Omega. \tag{2.3}$$

A typical example for just one phase is given via

$$\tilde{f}(\theta,\zeta) = \frac{1}{\tau_\zeta}[\zeta_{eq}(\theta) - \zeta]_+. \tag{2.4}$$

This model is derived from [5], where a transient model based on the Leblond-Devaux model is proposed that reproduces the relative volume fraction of the different solid phases of steel during a heating and cooling cycle.

To complete the PDE system, we need to impose boundary conditions on the faces of Ω. This way, we use Γ_N for the faces where we impose Neumann boundary conditions and Γ_D where a Dirichlet condition is imposed. Finally, to simplify the notation, the product ρC_p is substituted by $\tilde{\eta}$.

Thus, the governing equations read as

$$\tilde{\eta}(\theta)(\boldsymbol{v}\cdot\nabla)\theta - \nabla\cdot(\tilde{\kappa}(\theta)\nabla\theta) + \rho\boldsymbol{L}\cdot\tilde{\boldsymbol{f}}(\theta,\boldsymbol{\zeta}) = u\gamma \quad \text{in } \Omega, \tag{2.5a}$$

$$\boldsymbol{n}\cdot\tilde{\kappa}(\theta)\nabla\theta + h(\theta-\theta_0) = 0 \quad \text{on } \Gamma_N, \qquad \theta = \theta_0 \quad \text{on } \Gamma_D, \tag{2.5b}$$

$$(\boldsymbol{v}\cdot\nabla)\boldsymbol{\zeta} - \varepsilon\Delta\boldsymbol{\zeta} - \tilde{\boldsymbol{f}}(\theta,\boldsymbol{\zeta}) = \boldsymbol{0} \quad \text{in } \Omega, \tag{2.5c}$$

$$\boldsymbol{n}\cdot\nabla\boldsymbol{\zeta} = \boldsymbol{0} \quad \text{on } \Gamma_N, \qquad \boldsymbol{\zeta} = \boldsymbol{\zeta}_0 \quad \text{on } \Gamma_D. \tag{2.5d}$$

The vector $\boldsymbol{n}$ is an outward normal unit vector to the corresponding surface. We assume that $\boldsymbol{v}\cdot\boldsymbol{n} \geq 0$ on Γ_N that $\tilde{\eta}$ and $\tilde{\kappa}$ are sufficiently smooth and bounded from below and above, *i.e.*, $0 < c \leq \tilde{\eta}(r), \tilde{\kappa}(r) \leq C$ for two constants $c < C \in \mathbb{R}$.

Since the equation is rather transport dominated, we use the enthalpy transformation to get a linear transport term. We define $\eta(\theta) = \int_0^\theta \tilde{\eta}(r)\,\mathrm{d}r$. Note that the derivative $\eta' = \tilde{\eta}$ is well controlled from below and above, which assures that η is monotone and bijective such that η^{-1} is well defined and monotone, too. By defining $\vartheta := \eta(\theta)$ the equations can be reformulated for ϑ. With $\kappa(\vartheta) := \tilde{\kappa}(\eta^{-1}(\vartheta))/\tilde{\eta}(\eta^{-1}(\vartheta))$, $\boldsymbol{f}(\vartheta,\boldsymbol{\zeta}) := \tilde{\boldsymbol{f}}(\eta^{-1}(\vartheta),\boldsymbol{\zeta})$, and $g(\vartheta) := h\eta^{-1}(\vartheta)$, we find

$$(\boldsymbol{v}\cdot\nabla)\vartheta - \nabla\cdot(\kappa(\vartheta)\nabla\vartheta) + \rho\boldsymbol{L}\cdot\boldsymbol{f}(\vartheta,\boldsymbol{\zeta}) = u\gamma \quad \text{in } \Omega, \tag{2.6a}$$

$$\boldsymbol{n}\cdot\kappa(\vartheta)\nabla\vartheta + g(\vartheta) = 0 \quad \text{on } \Gamma_N, \qquad \vartheta = 0 \quad \text{on } \Gamma_D, \tag{2.6b}$$

$$(\boldsymbol{v}\cdot\nabla)\boldsymbol{\zeta} - \varepsilon\Delta\boldsymbol{\zeta} - \boldsymbol{f}(\vartheta,\boldsymbol{\zeta}) = \boldsymbol{0} \quad \text{in } \Omega, \tag{2.6c}$$

$$\boldsymbol{n}\cdot\nabla\boldsymbol{\zeta} = \boldsymbol{0} \quad \text{on } \Gamma_N, \qquad \boldsymbol{\zeta} = \boldsymbol{0} \quad \text{on } \Gamma_D. \tag{2.6d}$$

Note that, in order to reduce the notational complexity, we also normalized the Dirichlet boundary conditions to homogeneous ones. Therefore, we have to assume that θ_0 and $\boldsymbol{\zeta}_0$ are sufficiently smooth, i.e., $\theta_0 \in \boldsymbol{W}^{1-1/p,p}(\partial\Omega)$ and $\boldsymbol{\zeta}_0 \in H^{1/2}(\partial\Omega)^m$. See [11, Section 5.3] or [12, Proposition 3.31].

To simplify the notation in the next section, we will use Q to substitute the product of u and γ.

Notation: Throughout the manuscript we denote by Ω a bounded Lipschitz domain in dimension two and three. The boundary is assumed to have two parts $\partial\Omega = \Gamma_D \cup \Gamma_N$. The outer normal vector on the boundary is denoted by $\boldsymbol{n}$. Vectors are denoted in bold letters. We use the standard notation for Lebesgue and Sobolev spaces, *e.g.*, $L^p(\Omega)$, $W^{1,p}(\Omega)$ for $p \in [1,\infty]$. By $W^{1,p}_{\Gamma_D}(\Omega)$ we denote the Sobolev space with $f \in W^{1,p}(\Omega)$ such that $f = 0$ on Γ_D in the sense of the trace.

3 Existence, uniqueness, and regularity of the solutions to the state equations

Assumption 1. *We assume that* $\boldsymbol{v} \in \mathscr{C}^1(\Omega)^d$ *with* $\nabla\cdot\boldsymbol{v} = 0$, $\boldsymbol{n}\cdot\boldsymbol{v} \leq 0$ *on* Γ_D, *and* $\boldsymbol{n}\cdot\boldsymbol{v} \geq 0$ *on* Γ_N. *The function* $\kappa : \mathbb{R} \to \mathbb{R}$ *is bounded from below and above and Lipschitz continuous, i.e., there exists* $\underline{\kappa}, \overline{\kappa} \in \mathbb{R}$ *such that* $0 < \underline{\kappa} \leq \kappa(y) \leq \overline{\kappa}$ *for all* $y \in \mathbb{R}$ *and* $\kappa \in \mathscr{C}^1(\mathbb{R})$. *Let the functions* $g \in \mathscr{C}^1(\mathbb{R})$ *be monotone. We assume that the function* $\boldsymbol{f}$ *has the following form:* $\boldsymbol{f}(\vartheta,\boldsymbol{\zeta}) = \tilde{\boldsymbol{f}}(\boldsymbol{\zeta}_{eq}(\vartheta) - \boldsymbol{\zeta})$, *where* $\tilde{\boldsymbol{f}} : \mathbb{R}^m \to \mathbb{R}^m$ *with* $\tilde{\boldsymbol{f}} \in W^{1,\infty}(\mathbb{R}^m,\mathbb{R}^m)$ *and* $(D\tilde{\boldsymbol{f}})_{ij} = 0$ *for* $i \neq j$ *and* $(D\tilde{\boldsymbol{f}})_{ii} \geq 0$ *for all* i, $j \in \{1,\ldots,m\}$. *Additionally,* $\boldsymbol{\zeta}_{eq} \in (W^{1,\infty}(\mathbb{R},\mathbb{R}))^m$ *with* $\boldsymbol{\zeta}'_{eq_i} \geq 0$ *and* $\rho\boldsymbol{L}_i \geq 0$ *for* $i \in \{1,\ldots,m\}$.

Note that the derivatives are all defined in a generalized sense and the inequalities only holds almost everywhere.

Definition 2 (weak solution). *Let $p \in (3,6)$. For $Q \in W^{-1,p}_{\Gamma_D}(\Omega)$ the pair $(\vartheta, \boldsymbol{\zeta}) \in W^{1,p}_{\Gamma_D}(\Omega) \times H^1_{\Gamma_D}(\Omega)^m$ is a weak solution to system* (2.6)*, if*

$$\int_\Omega (\boldsymbol{v}\cdot\nabla)\vartheta\varphi + \kappa(\vartheta)\nabla\vartheta\cdot\nabla\varphi + \rho\boldsymbol{L}\cdot\boldsymbol{f}(\vartheta,\boldsymbol{z})\varphi\,d\boldsymbol{x} + \int_{\Gamma_N} g(\vartheta)\varphi\,dS = \int_\Omega Q\varphi\,d\boldsymbol{x}. \tag{3.1}$$

and

$$\int_\Omega (\boldsymbol{v}\cdot\nabla)\boldsymbol{\zeta}\cdot\boldsymbol{\psi} + \varepsilon\nabla\boldsymbol{\zeta} : \nabla\boldsymbol{\psi} - \boldsymbol{f}(\vartheta,\boldsymbol{\zeta})\cdot\boldsymbol{\psi}\,d\boldsymbol{x} = \boldsymbol{0} \tag{3.2}$$

are valid for all $\varphi \in W^{1,p'}_{\Gamma_D}(\Omega)$ with $1/p + 1/p' = 1$ and $\boldsymbol{\psi} \in H^1_{\Gamma_D}(\Omega)^m$.

Theorem 3. *Let the assumptions 1 be satisfied. Additionally, let $Q \in W^{-1,p}$ for $p \in (3,6)$. Then there exists a unique solution $(\vartheta, \boldsymbol{\zeta})$ to the system modelling laser beam shaping* (2.6) *in the sense of Definition* (2)*, which enjoys additional regularity, i.e., $\vartheta \in \mathscr{C}^\alpha(\Omega)$ for some $\alpha > 0$.*

Before we prove Theorem (3), we provide a comparison criterion, which will prove the uniqueness assertion of Theorem 3

Definition 4 (weak sub and super solution). *For $(Q, \boldsymbol{r}) \in \boldsymbol{H}^{-1}_{\Gamma_D}(\Omega) \times \boldsymbol{H}^{-1}_{\Gamma_D}(\Omega)^m$ and $\boldsymbol{a} \in L^2(\Omega)^d$ the pair $(\vartheta, \boldsymbol{\zeta}) \in \boldsymbol{H}^1_{\Gamma_D}(\Omega) \times \boldsymbol{H}^1_{\Gamma_D}(\Omega)^m$ is a weak sub (super) solution to system* (2.6)*, if*

$$\int_\Omega (\boldsymbol{v}\cdot\nabla)\vartheta\varphi + \kappa(\vartheta)\nabla\vartheta\cdot\nabla\varphi + \boldsymbol{L}\cdot\boldsymbol{f}(\vartheta,z)\varphi + \vartheta\boldsymbol{a}\cdot\nabla\varphi\,d\boldsymbol{x} + \int_{\Gamma_N} g(\vartheta)\varphi\,dS \le (\ge) \int_\Omega Q\varphi\,d\boldsymbol{x}. \tag{3.3}$$

and

$$\int_\Omega (\boldsymbol{v}\cdot\nabla)\boldsymbol{\zeta}_i\cdot\boldsymbol{\psi}_i + \varepsilon\nabla\boldsymbol{\zeta}_i\cdot\nabla\boldsymbol{\psi}_i - \boldsymbol{f}_i(\vartheta,\boldsymbol{\zeta})\boldsymbol{\psi}_i\,d\boldsymbol{x} \le (\ge) \int_\Omega \boldsymbol{r}_i\cdot\boldsymbol{\psi}_i \quad \text{for all } i \in \{0,\dots,m\} \tag{3.4}$$

are valid for all $\varphi \in H^1_{\Gamma_D}(\Omega)$ and $\boldsymbol{\psi} \in H^1_{\Gamma_D}(\Omega)^m$ with φ, $\boldsymbol{\psi}_i \ge 0$ a.e. on Ω for all $i \in \{0,\dots,m\}$.

Proposition 5. *Let Assumption 1 be fulfilled and let $\boldsymbol{a} \in L^2(\Omega)^d$. Let $(\underline{\vartheta}, \underline{\boldsymbol{\zeta}})$ be a sub solution and $(\overline{\vartheta}, \overline{\boldsymbol{\zeta}})$ a super solution according to Definition 4. Additionally, let $\underline{\vartheta} \le \overline{\vartheta}$ on Γ_D as well as $\underline{\boldsymbol{\zeta}}_i \le \overline{\boldsymbol{\zeta}}_i$ on Γ_D for $i \in \{1,\dots,m\}$. Then it holds $\underline{\vartheta} \le \overline{\vartheta}$ and $\underline{\boldsymbol{\zeta}}_i \le \overline{\boldsymbol{\zeta}}_i$ a.e. on Ω for $i \in \{1,\dots,m\}$.*

Proof. To show the comparison principle, we follow the argument used in Casas and Tröltzsch [6], which is originated in Křížek and Liu [9] and has also been used in Druet et al. [7]. Here we extend this technique to the considered case, which differs from the previous cases by being vector-valued, and due to the non-monotone transport term and the non-monotone nonlinearity $\boldsymbol{f}$.

We define the test functions $\theta^\delta := \min\{\delta, \max\{0, \underline{\vartheta} - \overline{\vartheta}\}\}$ and $\boldsymbol{\omega}^\delta_i := \min\{\delta, \max\{0, \rho\boldsymbol{L}_i(\underline{\boldsymbol{\zeta}}_i - \overline{\boldsymbol{\zeta}}_i)\}\}$. It holds $\theta^\delta \in H^1_{\Gamma_D}(\Omega)$, $\boldsymbol{\omega}^\delta \in H^1_{\Gamma_D}(\Omega)^m$, such that testing (3.3) with θ^δ and (3.4) with $\boldsymbol{\omega}^\delta$ is allowed. Adding both resulting equations for $(\underline{\vartheta}, \underline{\boldsymbol{\zeta}})$ and subtracting the sum of both equations for $(\overline{\vartheta}, \overline{\boldsymbol{\zeta}})$, we find

$$\int_\Omega (\boldsymbol{v}\cdot\nabla)(\underline{\vartheta} - \overline{\vartheta})\theta^\delta + \left(\kappa(\underline{\vartheta})\nabla\underline{\vartheta} - \kappa(\overline{\vartheta})\nabla\overline{\vartheta}\right)\cdot\nabla\theta^\delta + \varepsilon\nabla(\underline{\boldsymbol{\zeta}} - \overline{\boldsymbol{\zeta}}) : \nabla\boldsymbol{\omega}^\delta + (\boldsymbol{v}\cdot\nabla)(\underline{\boldsymbol{\zeta}} - \overline{\boldsymbol{\zeta}})\cdot\boldsymbol{\omega}^\delta\,\mathrm{d}\boldsymbol{x}$$
$$+ \int_{\Gamma_N} (g(\underline{\vartheta}) - g(\overline{\vartheta}))\theta^\delta\,\mathrm{d}S + \int_\Omega (\boldsymbol{f}(\underline{\vartheta}, \underline{\boldsymbol{\zeta}}) - \boldsymbol{f}(\overline{\vartheta}, \overline{\boldsymbol{\zeta}}))\cdot(\theta^\delta\rho\boldsymbol{L} - \boldsymbol{\omega}^\delta) + (\underline{\vartheta} - \overline{\vartheta})\boldsymbol{a}\cdot\nabla\theta^\delta\,\mathrm{d}\boldsymbol{x} \le 0$$

Integrating-by-parts the terms due to convection and ordering the terms, we observe

$$\int_{\partial\Omega}(\boldsymbol{v}\cdot\boldsymbol{n})\left((\underline{\vartheta}-\overline{\vartheta})\theta^\delta+((\underline{\boldsymbol{\zeta}}-\overline{\boldsymbol{\zeta}}))\cdot\boldsymbol{\omega}^\delta\right)\mathrm{d}S+\int_{\Gamma_N}(g(\underline{\vartheta})-g(\overline{\vartheta}))\theta^\delta\,\mathrm{d}S \tag{3.5a}$$

$$+\int_\Omega \kappa(\underline{\vartheta})(\nabla\underline{\vartheta}-\nabla\overline{\vartheta})\cdot\nabla\theta^\delta+\varepsilon(\nabla\underline{\boldsymbol{\zeta}}-\nabla\overline{\boldsymbol{\zeta}}):\nabla\boldsymbol{\omega}^\delta+(\boldsymbol{f}(\underline{\vartheta},\underline{\boldsymbol{\zeta}})-\boldsymbol{f}(\overline{\vartheta},\overline{\boldsymbol{\zeta}}))\cdot(\theta^\delta\rho\boldsymbol{L}-\boldsymbol{\omega}^\delta)\,\mathrm{d}\boldsymbol{x} \tag{3.5b}$$

$$\leq\int_\Omega(\underline{\vartheta}-\overline{\vartheta})(\boldsymbol{v}\cdot\nabla)\theta^\delta+(\underline{\boldsymbol{\zeta}}-\overline{\boldsymbol{\zeta}})\cdot(\boldsymbol{v}\cdot\nabla)\boldsymbol{\omega}^\delta-(\kappa(\underline{\vartheta})-\kappa(\overline{\vartheta}))\nabla\overline{\vartheta}\cdot\nabla\theta^\delta-(\underline{\vartheta}-\overline{\vartheta})\boldsymbol{a}\cdot\nabla\theta^\delta\,\mathrm{d}\boldsymbol{x}. \tag{3.5c}$$

Due to the assumptions on $\boldsymbol{v}$ on the boundary, the order of the elements on the Dirichlet part, and the monotony of g, all boundary terms in line (3.5a) are non-negative.

For every $\delta>0$, we introduce the sets

$$\Omega_0^\theta:=\{\boldsymbol{x}\in\Omega|\underline{\vartheta}(\boldsymbol{x})>\overline{\vartheta}(\boldsymbol{x})\},\qquad \Omega_\delta^\theta:=\{\boldsymbol{x}\in\Omega_0^\theta|\underline{\vartheta}(\boldsymbol{x})-\overline{\vartheta}(\boldsymbol{x})>\delta\}, \tag{3.6a}$$

$$\Omega_0^i:=\{\boldsymbol{x}\in\Omega|\underline{\boldsymbol{\zeta}}_i(\boldsymbol{x})>\overline{\boldsymbol{\zeta}}_i(\boldsymbol{x})\},\qquad \Omega_\delta^i:=\{\boldsymbol{x}\in\Omega_0^i|\rho\boldsymbol{L}_i(\underline{\boldsymbol{\zeta}}_i(\boldsymbol{x})-\overline{\boldsymbol{\zeta}}_i(\boldsymbol{x}))>\delta\}. \tag{3.6b}$$

We observe that $\Omega_\delta^\theta\nearrow\Omega_0^\theta$ and $\Omega_\delta^i\nearrow\Omega_0^i$ for $i\in\{1,\dots,m\}$ as $\delta\searrow 0$. Further, we observe that $\operatorname{supp}(\theta^\delta)=\Omega_0^\theta$ and $\operatorname{supp}(\boldsymbol{\omega}_i^\delta)=\Omega_0^i$ as well as $\operatorname{supp}(\nabla\theta^\delta)=\Omega_0^\theta/\Omega_\delta^\theta$ and $\operatorname{supp}(\nabla\boldsymbol{\omega}_i^\delta)=\Omega_0^i/\Omega_\delta^i$ for $i\in\{1,\dots,m\}$.

The last observation let us conclude that

$$\begin{aligned}\int_\Omega \kappa(\underline{\vartheta})(\nabla\underline{\vartheta}-\nabla\overline{\vartheta})\cdot\nabla\theta^\delta+\varepsilon(\nabla\underline{\boldsymbol{\zeta}}-\nabla\overline{\boldsymbol{\zeta}}):\nabla\boldsymbol{\omega}^\delta\,\mathrm{d}\boldsymbol{x}=&\int_{\Omega_0^\theta/\Omega_\delta^\theta}\kappa(\underline{\vartheta})|\nabla\theta^\delta|^2\,\mathrm{d}\boldsymbol{x}\\ &+\sum_{i=1}^m\int_{\Omega_0^i/\Omega_\delta^i}\varepsilon|\nabla\boldsymbol{\omega}_i^\delta|^2\,\mathrm{d}\boldsymbol{x}\\ &\geq\underline{\kappa}\|\nabla\theta^\delta\|_{L^2}^2+\varepsilon\|\nabla\boldsymbol{\omega}^\delta\|_{L^2}^2.\end{aligned} \tag{3.7}$$

Similarly, we find for the right-hand side (3.5c) that

$$\begin{aligned}&\int_\Omega(\underline{\vartheta}-\overline{\vartheta})(\boldsymbol{v}\cdot\nabla)\theta^\delta+(\underline{\boldsymbol{\zeta}}-\overline{\boldsymbol{\zeta}})\cdot(\boldsymbol{v}\cdot\nabla)\boldsymbol{\omega}^\delta-(\kappa(\underline{\vartheta})-\kappa(\overline{\vartheta}))\nabla\overline{\vartheta}\cdot\nabla\theta^\delta-(\underline{\vartheta}-\overline{\vartheta})\boldsymbol{a}\cdot\nabla\theta^\delta\,\mathrm{d}\boldsymbol{x}\\ &=\int_{\Omega_0^\theta/\Omega_\delta^\theta}(\underline{\vartheta}-\overline{\vartheta})(\boldsymbol{v}\cdot\nabla)\theta^\delta-(\kappa(\underline{\vartheta})-\kappa(\overline{\vartheta}))\nabla\overline{\vartheta}\cdot\nabla\theta^\delta-(\underline{\vartheta}-\overline{\vartheta})\boldsymbol{a}\cdot\nabla\theta^\delta\,\mathrm{d}\boldsymbol{x}\\ &\quad+\sum_{i=1}^m\int_{\Omega_0^i/\Omega_\delta^i}(\underline{\boldsymbol{\zeta}}_i-\overline{\boldsymbol{\zeta}}_i)(\boldsymbol{v}\cdot\nabla)\boldsymbol{\omega}_i^\delta\,\mathrm{d}\boldsymbol{x}\\ &\leq\delta(1+\|\kappa'\|_\infty)\left(\int_{\Omega_0^\theta/\Omega_\delta^\theta}|\boldsymbol{v}|^2+|\nabla\overline{\vartheta}|^2+|\boldsymbol{a}|^2\,\mathrm{d}\boldsymbol{x}\right)^{1/2}\|\nabla\theta^\delta\|_{L^2}\\ &\quad+\delta\sum_{i=1}^m\left(\int_{\Omega_0^i/\Omega_\delta^i}|\rho\boldsymbol{L}_i|^{-2}|\boldsymbol{v}|^2\,\mathrm{d}\boldsymbol{x}\right)^{1/2}\|\nabla\boldsymbol{\omega}_i^\delta\|_{L^2}.\end{aligned} \tag{3.8}$$

It remains to estimate the nonlinear coupling function $\boldsymbol{f}$. Inserting the definition of $\boldsymbol{f}$, we observe

$$\begin{aligned}(\boldsymbol{f}(\underline{\vartheta},\underline{\boldsymbol{\zeta}})-\boldsymbol{f}(\overline{\vartheta},\overline{\boldsymbol{\zeta}}))&=(\tilde{\boldsymbol{f}}(\boldsymbol{\zeta}_{\mathrm{eq}}(\underline{\vartheta})-\underline{\boldsymbol{\zeta}})-\tilde{\boldsymbol{f}}(\boldsymbol{\zeta}_{\mathrm{eq}}(\overline{\vartheta})-\overline{\boldsymbol{\zeta}}))\\ &=\sum_{i=1}^m\int_{(\boldsymbol{\zeta}_{\mathrm{eq}_i}(\overline{\vartheta})-\overline{\boldsymbol{\zeta}}_i)}^{(\boldsymbol{\zeta}_{\mathrm{eq}_i}(\underline{\vartheta})-\underline{\boldsymbol{\zeta}}_i)}(D\tilde{\boldsymbol{f}})_{ii}(s)\,\mathrm{d}s\left((\boldsymbol{\zeta}_{\mathrm{eq}_i}(\underline{\vartheta})-\boldsymbol{\zeta}_{\mathrm{eq}_i}(\overline{\vartheta}))-(\underline{\boldsymbol{\zeta}}_i-\overline{\boldsymbol{\zeta}}_i)\right)\end{aligned}$$

We define $\boldsymbol{h}_i := \int_{(\boldsymbol{\zeta}_{\mathrm{eq}_i}(\overline{\vartheta})-\overline{\boldsymbol{\zeta}}_i)}^{(\boldsymbol{\zeta}_{\mathrm{eq}_i}(\underline{\vartheta})-\underline{\boldsymbol{\zeta}}_i)} (D\tilde{\boldsymbol{f}})_{ii}(s)\,\mathrm{d}s$ and keep in mind that this function is non-negative according to Assumption 1. Using this generalized fundamental lemma of differential and integral calculus, we find for the considered term

$$
\begin{aligned}
&\int_\Omega (\boldsymbol{f}(\underline{\vartheta},\underline{\boldsymbol{\zeta}}) - \boldsymbol{f}(\overline{\vartheta},\overline{\boldsymbol{\zeta}}))\cdot(\theta^\delta\rho\boldsymbol{L} - \boldsymbol{\omega}^\delta)\,\mathrm{d}\boldsymbol{x}\\
&= \int_\Omega \sum_{i=1}^m \boldsymbol{h}_i \left((\boldsymbol{\zeta}_{\mathrm{eq}_i}(\underline{\vartheta}) - \boldsymbol{\zeta}_{\mathrm{eq}_i}(\overline{\vartheta})) - (\underline{\boldsymbol{\zeta}}_i - \overline{\boldsymbol{\zeta}}_i)\right)(\theta^\delta\rho\boldsymbol{L}_i - \boldsymbol{\omega}_i^\delta)\,\mathrm{d}\boldsymbol{x}\\
&= \int_\Omega \sum_{i=1}^m \boldsymbol{h}_i \left(\rho\boldsymbol{L}_i(\boldsymbol{\zeta}_{\mathrm{eq}_i}(\underline{\vartheta}) - \boldsymbol{\zeta}_{\mathrm{eq}_i}(\overline{\vartheta}))\theta^\delta + (\underline{\boldsymbol{\zeta}}_i - \overline{\boldsymbol{\zeta}}_i)\boldsymbol{\omega}_i^\delta\right)\mathrm{d}\boldsymbol{x}\\
&\quad - \int_\Omega \sum_{i=1}^m \boldsymbol{h}_i \left((\boldsymbol{\zeta}_{\mathrm{eq}_i}(\underline{\vartheta}) - \boldsymbol{\zeta}_{\mathrm{eq}_i}(\overline{\vartheta}))\boldsymbol{\omega}_i^\delta + (\underline{\boldsymbol{\zeta}}_i - \overline{\boldsymbol{\zeta}}_i)\theta^\delta\rho\boldsymbol{L}_i\right)\mathrm{d}\boldsymbol{x}
\end{aligned}
\tag{3.9}
$$

We consider the last line further on. Inserting the definitions of $\boldsymbol{\omega}^\delta$ and θ^δ, we may observe

$$
\begin{aligned}
&- \int_\Omega \sum_{i=1}^m \boldsymbol{h}_i \left((\boldsymbol{\zeta}_{\mathrm{eq}_i}(\underline{\vartheta}) - \boldsymbol{\zeta}_{\mathrm{eq}_i}(\overline{\vartheta}))\boldsymbol{\omega}_i^\delta + (\underline{\boldsymbol{\zeta}}_i - \overline{\boldsymbol{\zeta}}_i)\theta^\delta\rho\boldsymbol{L}_i\right)\mathrm{d}\boldsymbol{x}\\
&= -\sum_{i=1}^m \int_{\Omega_0^i} \boldsymbol{h}_i \left((\boldsymbol{\zeta}_{\mathrm{eq}_i}(\underline{\vartheta}) - \boldsymbol{\zeta}_{\mathrm{eq}_i}(\overline{\vartheta}))\boldsymbol{\omega}_i^\delta\right)\mathrm{d}\boldsymbol{x} - \sum_{i=1}^m \rho\boldsymbol{L}_i\boldsymbol{h}_i \int_{\Omega_0^\theta}\left(\underline{\boldsymbol{\zeta}}_i - \overline{\boldsymbol{\zeta}}_i\right)\theta^\delta\,\mathrm{d}\boldsymbol{x}\\
&\geq -\sum_{i=1}^m \int_{\Omega_0^i\cap\Omega_0^\theta} \boldsymbol{h}_i \left((\boldsymbol{\zeta}_{\mathrm{eq}_i}(\underline{\vartheta}) - \boldsymbol{\zeta}_{\mathrm{eq}_i}(\overline{\vartheta}))\boldsymbol{\omega}_i^\delta\right)\mathrm{d}\boldsymbol{x} - \sum_{i=1}^m \rho\boldsymbol{L}_i \int_{\Omega_0^\theta\cap\Omega_0^i}\boldsymbol{h}_i\left(\underline{\boldsymbol{\zeta}}_i - \overline{\boldsymbol{\zeta}}_i\right)\theta^\delta\,\mathrm{d}\boldsymbol{x},
\end{aligned}
$$

where the equality holds due to the support of the functions $\boldsymbol{\omega}_i^\delta$ and θ^δ and the inequality holds since the functions under the integral, i.e., $\boldsymbol{h}_i(\boldsymbol{\zeta}_{\mathrm{eq}_i}(\underline{\vartheta}) - \boldsymbol{\zeta}_{\mathrm{eq}_i}(\overline{\vartheta}))\boldsymbol{\omega}_i^\delta$ and $\boldsymbol{h}_i\left(\underline{\boldsymbol{\zeta}}_i - \overline{\boldsymbol{\zeta}}_i\right)\theta^\delta$, are negative on the sets $\Omega_0^i/\Omega_0^\theta$ and $\Omega_0^\theta/\Omega_0^i$, respectively. We further decompose the right-hand side, implying

$$
\begin{aligned}
&-\sum_{i=1}^m \int_{\Omega_0^i\cap\Omega_0^\theta} \boldsymbol{h}_i \left((\boldsymbol{\zeta}_{\mathrm{eq}_i}(\underline{\vartheta}) - \boldsymbol{\zeta}_{\mathrm{eq}_i}(\overline{\vartheta}))\boldsymbol{\omega}_i^\delta\right)\mathrm{d}\boldsymbol{x} - \sum_{i=1}^m \rho\boldsymbol{L}_i \int_{\Omega_0^\theta\cap\Omega_0^i}\boldsymbol{h}_i\left(\underline{\boldsymbol{\zeta}}_i - \overline{\boldsymbol{\zeta}}_i\right)\theta^\delta\,\mathrm{d}\boldsymbol{x}\\
&= -\sum_{i=1}^m \int_{\Omega_0^i\cap\Omega_0^\theta/\Omega_\delta^\theta} \boldsymbol{h}_i \left((\boldsymbol{\zeta}_{\mathrm{eq}_i}(\underline{\vartheta}) - \boldsymbol{\zeta}_{\mathrm{eq}_i}(\overline{\vartheta}))\boldsymbol{\omega}_i^\delta\right)\mathrm{d}\boldsymbol{x} - \sum_{i=1}^m \rho\boldsymbol{L}_i \int_{\Omega_0^\theta\cap\Omega_0^i/\Omega_\delta^i}\boldsymbol{h}_i\left(\underline{\boldsymbol{\zeta}}_i - \overline{\boldsymbol{\zeta}}_i\right)\theta^\delta\,\mathrm{d}\boldsymbol{x}\\
&\quad -\sum_{i=1}^m \int_{\Omega_0^i\cap\Omega_\delta^\theta} \boldsymbol{h}_i \left((\boldsymbol{\zeta}_{\mathrm{eq}_i}(\underline{\vartheta}) - \boldsymbol{\zeta}_{\mathrm{eq}_i}(\overline{\vartheta}))\boldsymbol{\omega}_i^\delta\right)\mathrm{d}\boldsymbol{x} - \sum_{i=1}^m \rho\boldsymbol{L}_i \int_{\Omega_0^\theta\cap\Omega_\delta^i}\boldsymbol{h}_i\left(\underline{\boldsymbol{\zeta}}_i - \overline{\boldsymbol{\zeta}}_i\right)\theta^\delta\,\mathrm{d}\boldsymbol{x}.
\end{aligned}
$$

We consider the last line of the previous equation, the definitions of $\boldsymbol{\omega}^\delta$ and θ^δ imply

$$
\begin{aligned}
&-\sum_{i=1}^m \int_{\Omega_0^i\cap\Omega_\delta^\theta} \boldsymbol{h}_i \left((\boldsymbol{\zeta}_{\mathrm{eq}_i}(\underline{\vartheta}) - \boldsymbol{\zeta}_{\mathrm{eq}_i}(\overline{\vartheta}))\boldsymbol{\omega}_i^\delta\right)\mathrm{d}\boldsymbol{x} - \sum_{i=1}^m \rho\boldsymbol{L}_i \int_{\Omega_0^\theta\cap\Omega_\delta^i}\boldsymbol{h}_i\left(\underline{\boldsymbol{\zeta}}_i - \overline{\boldsymbol{\zeta}}_i\right)\theta^\delta\,\mathrm{d}\boldsymbol{x}\\
&\geq -\sum_{i=1}^m \int_{\Omega_0^i\cap\Omega_\delta^\theta} \boldsymbol{h}_i \left((\boldsymbol{\zeta}_{\mathrm{eq}_i}(\underline{\vartheta}) - \boldsymbol{\zeta}_{\mathrm{eq}_i}(\overline{\vartheta}))\delta\right)\mathrm{d}\boldsymbol{x} - \sum_{i=1}^m \rho\boldsymbol{L}_i \int_{\Omega_0^\theta\cap\Omega_\delta^i}\boldsymbol{h}_i\left(\underline{\boldsymbol{\zeta}}_i - \overline{\boldsymbol{\zeta}}_i\right)\delta\,\mathrm{d}\boldsymbol{x}\\
&\geq -\sum_{i=1}^m \int_{\Omega_0^i\cap\Omega_\delta^\theta} \rho\boldsymbol{L}_i\boldsymbol{h}_i \left((\boldsymbol{\zeta}_{\mathrm{eq}_i}(\underline{\vartheta}) - \boldsymbol{\zeta}_{\mathrm{eq}_i}(\overline{\vartheta}))\theta^\delta\right)\mathrm{d}\boldsymbol{x} - \sum_{i=1}^m \int_{\Omega_0^\theta\cap\Omega_\delta^i}\boldsymbol{h}_i\left(\underline{\boldsymbol{\zeta}}_i - \overline{\boldsymbol{\zeta}}_i\right)\boldsymbol{\omega}_i^\delta\,\mathrm{d}\boldsymbol{x},
\end{aligned}
$$

since $\boldsymbol{\omega}_i^\delta \leq \rho\boldsymbol{L}_i\delta = \rho\boldsymbol{L}_i\theta^\delta$ on $\Omega_0^i\cap\Omega_\delta^\theta$ and $\rho\boldsymbol{L}_i\theta^\delta \leq \rho\boldsymbol{L}_i\delta = \boldsymbol{\omega}_i^\delta$ on $\Omega_0^\theta\cap\Omega_\delta^i$ for all $i\in\{1,\ldots,m\}$.

Inserting everything back into (3.9), we conclude

$$
\begin{aligned}
&\int_\Omega (\boldsymbol{f}(\underline{\vartheta},\underline{\boldsymbol{\zeta}}) - \boldsymbol{f}(\overline{\vartheta},\overline{\boldsymbol{\zeta}}))\cdot(\theta^\delta \rho \boldsymbol{L} - \boldsymbol{\omega}^\delta)\,\mathsf{d}\boldsymbol{x} \\
&\geq \sum_{i=1}^m \left(\int_{\Omega_0^\theta} \rho \boldsymbol{L}_i \boldsymbol{h}_i (\boldsymbol{\zeta}_{\mathsf{eq}_i}(\underline{\vartheta}) - \boldsymbol{\zeta}_{\mathsf{eq}_i}(\overline{\vartheta}))\theta^\delta \,\mathsf{d}\boldsymbol{x} + \int_{\Omega_0^i} \boldsymbol{h}_i(\underline{\boldsymbol{\zeta}}_i - \overline{\boldsymbol{\zeta}}_i)\boldsymbol{\omega}_i^\delta \,\mathsf{d}\boldsymbol{x} \right) \\
&\quad - \sum_{i=1}^m \int_{\Omega_0^i \cap \Omega_0^\theta/\Omega_\delta^\theta} \boldsymbol{h}_i \left((\boldsymbol{\zeta}_{\mathsf{eq}_i}(\underline{\vartheta}) - \boldsymbol{\zeta}_{\mathsf{eq}_i}(\overline{\vartheta}))\boldsymbol{\omega}_i^\delta \right) \mathsf{d}\boldsymbol{x} - \sum_{i=1}^m \rho \boldsymbol{L}_i \int_{\Omega_0^\theta \cap \Omega_0^i/\Omega_\delta^i} \boldsymbol{h}_i \left(\underline{\boldsymbol{\zeta}}_i - \overline{\boldsymbol{\zeta}}_i \right) \theta^\delta \,\mathsf{d}\boldsymbol{x} \\
&\quad - \sum_{i=1}^m \int_{\Omega_0^i \cap \Omega_\delta^\theta} \rho \boldsymbol{L}_i \boldsymbol{h}_i \left((\boldsymbol{\zeta}_{\mathsf{eq}_i}(\underline{\vartheta}) - \boldsymbol{\zeta}_{\mathsf{eq}_i}(\overline{\vartheta}))\theta^\delta \right) \mathsf{d}\boldsymbol{x} - \sum_{i=1}^m \int_{\Omega_0^\theta \cap \Omega_\delta^i} \boldsymbol{h}_i \left(\underline{\boldsymbol{\zeta}}_i - \overline{\boldsymbol{\zeta}}_i \right) \boldsymbol{\omega}_i^\delta \,\mathsf{d}\boldsymbol{x} \\
&\geq \sum_{i=1}^m \left(\int_{\Omega_0^\theta/(\Omega_0^i \cap \Omega_\delta^\theta)} \rho \boldsymbol{L}_i \boldsymbol{h}_i (\boldsymbol{\zeta}_{\mathsf{eq}_i}(\underline{\vartheta}) - \boldsymbol{\zeta}_{\mathsf{eq}_i}(\overline{\vartheta}))\theta^\delta \,\mathsf{d}\boldsymbol{x} + \int_{\Omega_0^i/(\Omega_0^\theta \cap \Omega_\delta^i)} \boldsymbol{h}_i(\underline{\boldsymbol{\zeta}}_i - \overline{\boldsymbol{\zeta}}_i)\boldsymbol{\omega}_i^\delta \,\mathsf{d}\boldsymbol{x} \right) \\
&\quad - \sum_{i=1}^m \int_{\Omega_0^i \cap \Omega_0^\theta/\Omega_\delta^\theta} \boldsymbol{h}_i \left((\boldsymbol{\zeta}_{\mathsf{eq}_i}(\underline{\vartheta}) - \boldsymbol{\zeta}_{\mathsf{eq}_i}(\overline{\vartheta}))\boldsymbol{\omega}_i^\delta \right) \mathsf{d}\boldsymbol{x} - \sum_{i=1}^m \rho \boldsymbol{L}_i \int_{\Omega_0^\theta \cap \Omega_0^i/\Omega_\delta^i} \boldsymbol{h}_i \left(\underline{\boldsymbol{\zeta}}_i - \overline{\boldsymbol{\zeta}}_i \right) \theta^\delta \,\mathsf{d}\boldsymbol{x}.
\end{aligned}
$$

The first line on the right-hand side of the previous inequality is non-negative such that we can estimate it from below by zero. Estimating the other terms appropriately, we find

$$
\begin{aligned}
&\int_\Omega (\boldsymbol{f}(\underline{\vartheta},\underline{\boldsymbol{\zeta}}) - \boldsymbol{f}(\overline{\vartheta},\overline{\boldsymbol{\zeta}}))\cdot(\theta^\delta \rho \boldsymbol{L} - \boldsymbol{\omega}^\delta)\,\mathsf{d}\boldsymbol{x} \\
&\geq -\sum_{i=1}^m \int_{\Omega_0^i \cap \Omega_0^\theta/\Omega_\delta^\theta} \boldsymbol{h}_i \left((\boldsymbol{\zeta}_{\mathsf{eq}_i}(\underline{\vartheta}) - \boldsymbol{\zeta}_{\mathsf{eq}_i}(\overline{\vartheta}))\boldsymbol{\omega}_i^\delta \right) \mathsf{d}\boldsymbol{x} - \sum_{i=1}^m \rho \boldsymbol{L}_i \int_{\Omega_0^\theta \cap \Omega_0^i/\Omega_\delta^i} \boldsymbol{h}_i \left(\underline{\boldsymbol{\zeta}}_i - \overline{\boldsymbol{\zeta}}_i \right) \theta^\delta \,\mathsf{d}\boldsymbol{x} \\
&\geq -\delta \|\boldsymbol{\zeta}_{\mathsf{eq}}'\|_\infty \sum_{i=1}^m \left(\int_{\Omega_0^i \cap \Omega_0^\theta/\Omega_\delta^\theta} \left(\max_i \boldsymbol{h}_i \right)^2 \mathsf{d}\boldsymbol{x} \right)^{1/2} \|\boldsymbol{\omega}_i^\delta\|_{L^2} \\
&\quad - \delta \sum_{i=1}^m \left(\int_{\Omega_0^\theta \cap \Omega_0^i/\Omega_\delta^i} (\max_i \boldsymbol{h}_i)^2 \right)^{1/2} \|\theta^\delta\|_{L^2}.
\end{aligned}
\tag{3.10}
$$

Collecting now the estimates (3.7), (3.8), and (3.10) and combining them with (3.5) implies

$$
\begin{aligned}
\underline{\kappa}\|\nabla\theta^\delta\|_{L^2}^2 + \varepsilon\|\nabla\boldsymbol{\omega}^\delta\|_{L^2}^2 &\leq \delta(1+\|\kappa'\|_\infty)\left(\int_{\Omega_0^\theta/\Omega_\delta^\theta} |\boldsymbol{v}|^2 + |\nabla\overline{\vartheta}|^2 + |\boldsymbol{a}|^2 \,\mathsf{d}\boldsymbol{x} \right)^{1/2} \|\nabla\theta^\delta\|_{L^2} \\
&\quad + \delta \sum_{i=1}^m \left(\int_{\Omega_0^i/\Omega_\delta^i} \rho^2 L_i^2 |\boldsymbol{v}|^2 \,\mathsf{d}\boldsymbol{x} \right)^{1/2} \|\nabla\boldsymbol{\omega}_i^\delta\|_{L^2} \\
&\quad + \delta \|\boldsymbol{\zeta}_{\mathsf{eq}}'\|_\infty \sum_{i=1}^m \left(\int_{\Omega_0^i \cap \Omega_0^\theta/\Omega_\delta^\theta} \left(\max_i \boldsymbol{h}_i \right)^2 \mathsf{d}\boldsymbol{x} \right)^{1/2} \|\boldsymbol{\omega}_i^\delta\|_{L^2} \\
&\quad + \delta \sum_{i=1}^m \left(\int_{\Omega_0^\theta \cap \Omega_0^i/\Omega_\delta^i} (\max_i \boldsymbol{h}_i)^2 \right)^{1/2} \|\theta^\delta\|_{L^2}.
\end{aligned}
$$

Poincaré's inequality now let us conclude

$$
\begin{aligned}
&\operatorname{meas}(\Omega_\delta^\theta)+\sum_{i=1}^m \operatorname{meas}(\Omega_\delta^i)\\
&\quad\le \frac{1}{\delta}\left(\left(\int_{\Omega_\delta^\theta}\delta^2\,\mathrm{d}\boldsymbol{x}\right)^{1/2}+\sum_{i=1}^m\left(\int_{\Omega_\delta^i}\rho^2 L_i^2\delta^2\,\mathrm{d}\boldsymbol{x}\right)^{1/2}\right)\\
&\quad\le \frac{1}{\delta}\left(\|\theta^\delta\|_{L^2}+\|\omega^\delta\|_{L^2}\right)\\
&\quad\le c\frac{1}{\delta}\left(\underline{\kappa}\|\nabla\theta^\delta\|_{L^2}+\varepsilon\|\nabla\omega^\delta\|_{L^2}\right)\\
&\quad\le c\left(\int_{\Omega_0^\theta/\Omega_\delta^\theta}|\boldsymbol{v}|^2+|\nabla\overline{\vartheta}|^2+|\boldsymbol{a}|^2\,\mathrm{d}\boldsymbol{x}\right)^{1/2}+c\sum_{i=1}^m\left(\int_{\Omega_0^i/\Omega_\delta^i}\rho^2\boldsymbol{L}_i^2|\boldsymbol{v}|^2\,\mathrm{d}\boldsymbol{x}\right)^{1/2}\\
&\qquad+c\sum_{i=1}^m\left(\int_{\Omega_0^i\cap\Omega_0^\theta/\Omega_\delta^\theta}\left(\max_i h_i\right)^2\mathrm{d}\boldsymbol{x}\right)^{1/2}+c\sum_{i=1}^m\left(\int_{\Omega_0^\theta\cap\Omega_0^i/\Omega_\delta^i}(\max_i h_i)^2\right)^{1/2}.
\end{aligned}
$$

The integrability of $\boldsymbol{v}$, $\nabla\overline{\vartheta}$, $\boldsymbol{a}$, and $(\max_i \boldsymbol{h}_i)$ grants that the right-hand side of the previous inequality vanishes as $\delta\to 0$. This let us conclude that $\operatorname{meas}(\Omega_\delta^\theta)+\sum_{i=1}^m\operatorname{meas}(\Omega_\delta^i)\to 0$ as $\delta\to 0$ which implies $\operatorname{meas}(\Omega_0^\theta)+\sum_{i=1}^m\operatorname{meas}(\Omega_0^i)=0$ and therewith, the assertion. $\square$

Now, after having provided a comparison criterion useful for the uniqueness stated in Theorem 3, we go back to the proof of Theorem 3 which asserts the existence and uniqueness of a weak solution (Def. 2) of the system (2.6).

Proof. Existence: We want to employ a fixed-point technique based on Schauder's fixed point. Therefore, we define the mapping

$$\mathscr{T}: L_R^2\to L_R^2,\quad \text{where } L_R^2:=\{u\in L^2(\Omega);\|u\|_{L^2}\le R\}.$$

The operator $\mathscr{T}$ maps $(\overline{\vartheta})$ to the solution ϑ of the system

$$
\begin{aligned}
(\boldsymbol{v}\cdot\nabla)\vartheta-\nabla\cdot(\kappa(\vartheta)\nabla\vartheta)+\rho\boldsymbol{L}\cdot\boldsymbol{f}(\vartheta,\boldsymbol{\zeta})&=Q &&\text{in }\Omega, &&(3.11a)\\
\boldsymbol{n}\cdot\kappa(\vartheta)\nabla\vartheta&=g(\vartheta) &&\text{on }\Gamma_N, &&(3.11b)\\
\vartheta&=0 &&\text{on }\Gamma_D, &&(3.11c)\\
(\boldsymbol{v}\cdot\nabla)\boldsymbol{\zeta}-\varepsilon\Delta\boldsymbol{\zeta}-\boldsymbol{f}(\overline{\vartheta},\boldsymbol{\zeta})&=\boldsymbol{0} &&\text{in }\Omega, &&(3.11d)\\
\boldsymbol{n}\cdot\nabla\boldsymbol{\zeta}&=\boldsymbol{0} &&\text{on }\Gamma_N, &&(3.11e)\\
\boldsymbol{\zeta}&=\boldsymbol{0} &&\text{on }\Gamma_D. &&(3.11f)
\end{aligned}
$$

Note that the coupling between both is removed in the sense that we can now first solve (3.11d) to attain $\boldsymbol{\zeta}$ and insert this function in (3.11a) in order to find ϑ, the image of the mapping $\mathscr{T}$. Considering the operator $\mathscr{A}_{\overline{\vartheta}}$ associated to (3.11d),

$$\langle\mathscr{A}_{\overline{\vartheta}}(\boldsymbol{\zeta}),\boldsymbol{\psi}\rangle:=\int_\Omega(\boldsymbol{v}\cdot\nabla)\boldsymbol{\zeta}\cdot\boldsymbol{\psi}+\varepsilon\nabla\boldsymbol{\zeta}:\nabla\boldsymbol{\psi}-\boldsymbol{f}(\overline{\vartheta},\boldsymbol{\zeta})\cdot\boldsymbol{\psi}\,\mathrm{d}\boldsymbol{x}. \tag{3.12}$$

It is a routine matter to show that $\mathscr{A}_{\overline{\vartheta}}: H^1_{\Gamma_D}(\Omega)^m\to(H^1_{\Gamma_D}(\Omega)^m)^*$ is a continuous and pseudomonotone mapping.

Additionally, using $\varphi = \vartheta$ as test function in (3.12), we may infer

$$\begin{aligned}\langle \mathscr{A}_{\overline{\vartheta}}(\boldsymbol{\zeta}), \boldsymbol{\zeta}\rangle &= \int_\Omega (\boldsymbol{v}\cdot\nabla)\boldsymbol{\zeta}\cdot\boldsymbol{\zeta} + \varepsilon\nabla\boldsymbol{\zeta} : \nabla\boldsymbol{\zeta} - \boldsymbol{f}(\overline{\vartheta}, \boldsymbol{\zeta})\cdot\boldsymbol{\zeta}\,\mathrm{d}\boldsymbol{x} \\ &= \int_\Omega \frac{1}{2}(\boldsymbol{v}\cdot\nabla)|\boldsymbol{\zeta}|^2 + \varepsilon|\nabla\boldsymbol{\zeta}|^2 - \tilde{\boldsymbol{f}}(-\boldsymbol{\zeta})\cdot\boldsymbol{\zeta} - \boldsymbol{\zeta}_{\mathrm{eq}}(\overline{\vartheta})\int_0^1 D\tilde{\boldsymbol{f}}(-\boldsymbol{\zeta} + s\boldsymbol{\zeta}_{\mathrm{eq}}(\overline{\vartheta}))\,\mathrm{d}s\,\boldsymbol{\zeta}\,\mathrm{d}\boldsymbol{x} \\ &\geq \int_{\Gamma_N} \frac{1}{2}\boldsymbol{v}\cdot\boldsymbol{n}|\boldsymbol{\zeta}|^2\,\mathrm{d}S + \varepsilon\int_\Omega |\nabla\boldsymbol{\zeta}|^2\,\mathrm{d}\boldsymbol{x} - C\int_\Omega |\boldsymbol{\zeta}|\,\mathrm{d}\boldsymbol{x}.\end{aligned}$$

that $\mathscr{A}_{\overline{\vartheta}}$ is coercive, which guarantees that $\mathscr{A}_{\overline{\vartheta}}$ is surjective. Additionally, we find a constant such that $\|\boldsymbol{\zeta}\|_{H^1_{\Gamma_D}} \leq C$ for any $\overline{\vartheta} \in L^2_R$. The inequality is achieved by applying an integration-by-parts formula

$$\int_\Omega \frac{1}{2}(\boldsymbol{v}\cdot\nabla)|\boldsymbol{\zeta}|^2\,\mathrm{d}\boldsymbol{x} = \int_{\Gamma_N}\frac{1}{2}\boldsymbol{v}\cdot\boldsymbol{n}|\boldsymbol{\zeta}|^2\,\mathrm{d}S - \int_\Omega \frac{1}{2}\mathrm{div}\,\boldsymbol{v}|\boldsymbol{\zeta}|^2\,\mathrm{d}\boldsymbol{x} \tag{3.13}$$

and the fundamental theorem of differentiation and integration on $\tilde{\boldsymbol{f}}$

$$\tilde{\boldsymbol{f}}(\boldsymbol{\zeta}_{eq}(\overline{\vartheta}) - \boldsymbol{\zeta}) - \tilde{\boldsymbol{f}}(-\boldsymbol{\zeta}) = \boldsymbol{\zeta}_{\mathrm{eq}}(\overline{\vartheta})\int_0^1 D\tilde{\boldsymbol{f}}(s\boldsymbol{\zeta}_{\mathrm{eq}}(\overline{\vartheta}) - \boldsymbol{\zeta})\,\mathrm{d}s. \tag{3.14}$$

Note that this formula is valid due to the weak differentiability of $\tilde{\boldsymbol{f}}$. The uniqueness of solutions to (3.11d) is a consequence of the monotonicity of $\tilde{\boldsymbol{f}}$.

To show the continuity of the mapping $\mathscr{T}$, we consider the operator $\mathscr{H}_{\boldsymbol{\zeta}} : H^1_{\Gamma_D}(\Omega) \to H^{-1}_{\Gamma_D}(\Omega)$ given by

$$\langle \mathscr{H}_{\boldsymbol{\zeta}}(\vartheta), \varphi\rangle := \int_\Omega (\boldsymbol{v}\cdot\nabla)\vartheta\varphi + \kappa(\vartheta)\nabla\vartheta\cdot\nabla\varphi + \rho\boldsymbol{L}\cdot\boldsymbol{f}(\vartheta, \boldsymbol{\zeta})\varphi\,\mathrm{d}\boldsymbol{x} + \int_{\Gamma_N} g(\vartheta)\varphi\,\mathrm{d}S. \tag{3.15}$$

This operator is bijective, i.e., for every $Q \in H^{-1}_{\Gamma_D}$ there exists a unique solution $\vartheta \in H^1_{\Gamma_D}$ such that $\mathscr{H}_{\boldsymbol{\zeta}}(\vartheta) = Q$ in $H^{-1}_{\Gamma_D}$. Indeed, the existence follows from standard arguments concerning pseudomonotone mappings (see for instance Roubíček [13, Thm. 2.36]). Here, we only concentrate on the coercivity of the operator, since the pseudomonotony is fairly standard. Using $\varphi = \vartheta$ as test function in (3.15), we may infer

$$\begin{aligned}\langle \mathscr{H}_{\boldsymbol{\zeta}}(\vartheta), \vartheta\rangle &= \int_\Omega \frac{1}{2}(\boldsymbol{v}\cdot\nabla)|\vartheta|^2 + \kappa(\vartheta)|\nabla\vartheta|^2 + \rho\boldsymbol{L}\cdot\boldsymbol{f}(\vartheta, \boldsymbol{\zeta})\vartheta\,\mathrm{d}\boldsymbol{x} + \int_{\Gamma_N} g(\vartheta)\vartheta\,\mathrm{d}S \\ &\geq \int_\Omega \kappa(\vartheta)|\nabla\vartheta|^2 + \rho\boldsymbol{L}\tilde{\boldsymbol{f}}(\boldsymbol{\zeta}_{\mathrm{eq}}(\vartheta))\vartheta - \rho\boldsymbol{L}\cdot\int_0^1 D\tilde{\boldsymbol{f}}(\boldsymbol{\zeta}_{\mathrm{eq}}(\vartheta) - s\boldsymbol{\zeta})\,\mathrm{d}s\,\boldsymbol{\zeta}\vartheta\,\mathrm{d}\boldsymbol{x} \\ &\quad + \int_{\Gamma_N} g(\vartheta)\vartheta + \frac{1}{2}\boldsymbol{v}\cdot\boldsymbol{n}|\vartheta|^2\,\mathrm{d}S \\ &\geq \frac{\kappa}{2}\|\nabla\vartheta\|^2_{L^2} - C\|\boldsymbol{\zeta}\|^2_{L^2}.\end{aligned}$$

The first inequality may be observed by applying an integration-by-parts formula as in (3.13) and the fundamental theorem of differentiation and integration on $\tilde{\boldsymbol{f}}$ similar to (3.14) as

$$\tilde{\boldsymbol{f}}(\boldsymbol{\zeta}_{eq}(\vartheta) - \boldsymbol{\zeta}) - \tilde{\boldsymbol{f}}(\zeta_{eq}(\vartheta) = -\zeta\int_0^1 D\tilde{\boldsymbol{f}}(\boldsymbol{\zeta}_{\mathrm{eq}}(\vartheta) - s\boldsymbol{\zeta})\,\mathrm{d}s. \tag{3.16}$$

The second inequality follows from the monotony of g as well as the condition $\boldsymbol{v}\cdot\boldsymbol{n} \geq 0$ on Γ_N and the boundedness of $\nabla\tilde{\boldsymbol{f}}$ and that $\delta\|\vartheta\|^2_{L^2}$ can be absorbed into the leading order term for δ small enough.

The uniqueness of solutions to (3.11) follows from similar (but simpler) arguments as the uniqueness of the full system (see Proposition 5).

The mapping $\mathscr{T}$ is well defined, i.e. maps into L^2_R, for R big enough follows from the previous estimate, the bound we found on $\boldsymbol{\zeta}$, and the boundedness of q in L^2.

The continuity of $\mathscr{T}$ follows from the continuity of the solution operators $\mathscr{A}_{\overline{\vartheta}}$ and $\mathscr{H}_{\boldsymbol{\zeta}}$. Since $H^1_{\Gamma_D}$ is compactly embedded into L^2, Schauder's fixed point theorem assures the existence of a solution to the coupled system in the sense of Definition 2.

Regularity: In order to prove that the solution has the asserted regularity, we cite different results from the literature. Concerning the Hölder regularity, we observe that the energy balance can be written as

$$-\nabla\cdot(\kappa(\vartheta(\boldsymbol{x}))\nabla\vartheta) = F \quad \text{in } W^{-1,p}_{\Gamma_D} \quad \text{for } p>3$$

where the right-hand side F is given by

$$\langle F,\varphi\rangle = -\int_\Omega (\boldsymbol{v}\cdot\nabla)\vartheta\varphi + \rho\boldsymbol{L}\cdot\boldsymbol{f}(\vartheta,\boldsymbol{\zeta})\varphi\,\mathrm{d}\boldsymbol{x} - \int_{\Gamma_N} g(\vartheta)\varphi\,\mathrm{d}S + \int_\Omega Q\varphi\,\mathrm{d}\boldsymbol{x}.$$

This functional may be estimated by

$$|\langle F,\varphi\rangle| \le c\left(|\boldsymbol{v}|\|\nabla\vartheta\|_{L^2} + |\rho\boldsymbol{L}|\|\boldsymbol{f}(\vartheta,\boldsymbol{\zeta})\|_{L^2} + \|g(\vartheta)\|_{W^{-1/p,p}(\Gamma_N)} + \|Q\|_{W^{-1,p}}\right)\|\varphi\|_{W^{1,p'}}, \tag{3.17}$$

where $p' = p/(p-1)$. We used the embeddings

$$W^{1,p'}_{\Gamma_D}(\Omega) \hookrightarrow L^2(\Omega) \text{ and } W^{1,p'}(\Omega) \hookrightarrow W^{1-1/p',p'}(\Gamma_N) = W^{1/p,p'}(\Gamma_N)$$

for $p\in(3,6)$, i.e., $p'\in(6/5,3/2)$. The result in [14] provides the Hölder continuity of the solution $\vartheta \in \mathscr{C}^{0,\alpha}(\Omega)$ for some $\alpha>0$.

Uniqueness: The uniqueness follows from Proposition 5 with $\boldsymbol{a}=0$. Indeed, the comparison criterion implies that ϑ is unique and also $\rho\boldsymbol{L}\cdot\boldsymbol{\zeta}$. Since $\boldsymbol{\zeta}=\boldsymbol{0}$ is always a sub solution to equation (3.2), $\boldsymbol{\zeta}_i$ is non-negative. Due to the monotony of $-\boldsymbol{f}$ in $\boldsymbol{\zeta}$, the uniqueness of $\boldsymbol{\zeta}$ follows from equation (3.2) for a given unique ϑ. $\square$

Corollary 6. *The solution operator $\mathscr{S}: W^{-1,p}_{\Gamma_D}(\Omega)\to W^{1,p}_{\Gamma_D}(\Omega)\times H^1_{\Gamma_D}(\Omega)^m$ mapping q to a solution according to Definition 2 is even continuous, i.e., $Q_n\to Q$ in $W^{-1,p}_{\Gamma_D}(\Omega)$ implies $\mathscr{S}(Q_n)\to\mathscr{S}(Q)$ in $W^{1,p}_{\Gamma_D}(\Omega)\times H^1_{\Gamma_D}(\Omega)^m$.*

4 Linearised state equation

Assumption 7. *There exists a $M>0$ such that $|\kappa'(y)|\le M$ for all $y\in\mathbb{R}$. The function $\boldsymbol{f}$ is directional differentiable everywhere and we denote the directional derivative of $\boldsymbol{f}$ at y^* in direction y via $\boldsymbol{f}'(y^*;y)$.*

Remark 8 (Directional vs. weak differentiability)**.** *Up to now, we only used that the function $\boldsymbol{f}$ is weakly differentiable. In order to derive a variational inequality, we also use the directional differentiability. Since the nonlinearity is not continuosly differentiable, standard arguments to derive the adjiont system via an generalized inverse function theorem are not applicable here. But with the directional differentiability, we can also include the information of the variational inequality in the optimality conditions (see Theorem 13).*

We will switch between the writing of the directional derivative and the weak derivative.

Theorem 9. *Let* $(\vartheta^*, \boldsymbol{\zeta}^*)$ *be given and* $p \in (3,6)$. *For every* $(w, \boldsymbol{r}) \in H^{-1}_{\Gamma_D}(\Omega)^{m+1}$ *there exists a unique solution* $(\vartheta, \boldsymbol{\zeta}) \in H^1_{\Gamma_D}(\Omega)^{m+1}$ *to the linearised state equations*

$$
\begin{aligned}
(\boldsymbol{v}\cdot\nabla)\vartheta - \nabla\cdot(\kappa(\vartheta^*)\nabla\vartheta + \kappa'(\vartheta^*)\vartheta\nabla\vartheta^*) + \rho \boldsymbol{L}\cdot \boldsymbol{f}'(\vartheta^*,\boldsymbol{\zeta}^*;\vartheta,\boldsymbol{\zeta}) &= w && \text{in } \Omega, && (4.1a)\\
\boldsymbol{n}\cdot\kappa(\vartheta^*)\nabla\vartheta + \kappa'(\vartheta^*)\vartheta\nabla\vartheta^* &= g'(\vartheta^*)\vartheta && \text{on } \Gamma_N, && (4.1b)\\
\vartheta &= 0 && \text{on } \Gamma_D, && (4.1c)\\
(\boldsymbol{v}\cdot\nabla)\boldsymbol{\zeta} - \varepsilon\Delta\boldsymbol{\zeta} - \boldsymbol{f}'(\vartheta^*,\boldsymbol{\zeta}^*;\boldsymbol{\zeta},\vartheta) &= \boldsymbol{r} && \text{in } \Omega, && (4.1d)\\
\boldsymbol{n}\cdot\nabla\boldsymbol{\zeta} &= \boldsymbol{0} && \text{on } \Gamma_N, && (4.1e)\\
\boldsymbol{\zeta} &= \boldsymbol{0} && \text{on } \Gamma_D. && (4.1f)
\end{aligned}
$$

Additionally, the image of the solution operator is $(H^1_{\Gamma_D}(\Omega))^{m+1}$.

Proof. First, we prove that the solution operator associated to the linear part of (4.1) with $\boldsymbol{f} \equiv 0$ is a linear bounded bijective operator $\mathscr{T} : (H^{-1}_{\Gamma_D})^{m+1} \to (H^1_{\Gamma_D})^{m+1}$. Then we apply again Schauder's Fixed point theorem in order to deduce the existence of a solution to the full system.

The *existence for the linear part* follows from the linearity of the equation, the uniqueness and Fredholm's theorem.

We are going to split the equation into parts, the main part and the compact perturbations Therefore, we introduce the operator $\mathscr{A}(\vartheta^*, \boldsymbol{\zeta}^*) : (H^1_{\Gamma_D})^{m+1} \to (H^{-1}_{\Gamma_D})^{m+1}$ via

$$
\langle \mathscr{A}(\vartheta^*,\boldsymbol{\zeta}^*)(\vartheta,\boldsymbol{\zeta}),(\varphi,\boldsymbol{\psi})\rangle = \int_\Omega \kappa(\vartheta^*)\nabla\vartheta\cdot\nabla\varphi + \varepsilon\nabla\boldsymbol{\zeta} : \nabla\boldsymbol{\psi}\,\mathrm{d}\boldsymbol{x} + \int_{\Gamma_N} g'(\vartheta^*)\vartheta\varphi\,\mathrm{d}\boldsymbol{x}
$$

and the operator $\mathscr{B}(\vartheta^*, \boldsymbol{\zeta}^*) : (L^{2p/(p-2)}(\Omega))^{m+1} \to (H^{-1}_{\Gamma_D})^{m+1}$ via

$$
\begin{aligned}
\left\langle \mathscr{B}(\vartheta^*,\boldsymbol{\zeta}^*)(\vartheta,\boldsymbol{\zeta}),(\varphi,\boldsymbol{\psi})\right\rangle = &\int_\Omega \kappa'(\vartheta^*)\vartheta\nabla\vartheta^*\cdot\nabla\varphi - (\boldsymbol{v}\cdot\nabla)\varphi\vartheta - (\boldsymbol{v}\cdot\nabla)\boldsymbol{\psi}\cdot\boldsymbol{\zeta}\,\mathrm{d}\boldsymbol{x}\\
&+ \int_\Omega D\boldsymbol{f}(\vartheta^*,\zeta^*)\begin{pmatrix}\vartheta\\ \zeta\end{pmatrix}\cdot\begin{pmatrix}\varphi\\ \psi\end{pmatrix}\mathrm{d}\boldsymbol{x}
\end{aligned}
$$

as well as the boundary part operator $\mathscr{C}(\vartheta^*, \boldsymbol{\zeta}^*) : (L^2(\Gamma_N))^{m+1} \to (H^{-1}_{\Gamma_D})^{m+1}$

$$
\left\langle \mathscr{C}(\vartheta^*,\boldsymbol{\zeta}^*)(\vartheta,\boldsymbol{\zeta}),(\varphi,\boldsymbol{\psi})\right\rangle = \int_{\Gamma_N} (\boldsymbol{v}\cdot\boldsymbol{n})(\varphi\vartheta + \boldsymbol{\zeta}\cdot\boldsymbol{\psi})\,\mathrm{d}S
$$

as well as the compact embedding operators

$$
j : H^1_{\Gamma_D}(\Omega) \to L^{2p/(p-2)}(\Omega) \text{ as well as } j_{\mathrm{tr}} : H^1_{\Gamma_D}(\Omega) \to L^2(\Gamma_N)\,.
$$

These operators are well defined , i.e., for $\mathscr{B}$ we observe

$$
\begin{aligned}
&\int_\Omega \kappa'(\vartheta^*)\vartheta\nabla\vartheta^*\cdot\nabla\varphi - (\boldsymbol{v}\cdot\nabla)\varphi\vartheta - (\boldsymbol{v}\cdot\nabla)\boldsymbol{\psi}\cdot\boldsymbol{\zeta}\\
&\qquad\le c\left(\|\vartheta\|_{L^{2p/(p-2)}}\|\nabla\vartheta^*\|_{L^p}\|\nabla\varphi\|_{L^2} + \|\nabla\varphi\|_{L^2}\|\vartheta\|_{L^2} + \|\nabla\boldsymbol{\psi}\|_{L^2}\|\boldsymbol{\zeta}\|_{L^2}\right).
\end{aligned}
$$

For every $h \in (H^{-1}_{\Gamma_D})^{m+1}$ the system (4.1) can now be expressed as the operator equation

$$
\left(\mathscr{A}(\vartheta^*,\boldsymbol{\zeta}^*) + \mathscr{B}(\vartheta^*,\boldsymbol{\zeta}^*)\circ j + \mathscr{C}(\vartheta^*,\boldsymbol{\zeta}^*)\circ j_{\mathrm{tr}}\right) y = h \qquad \text{in } H^{-1}_{\Gamma_D}(\Omega)^{m+1}, \tag{4.2}
$$

with $y=(\vartheta,\boldsymbol{\zeta})\in(H^1_{\Gamma_D})^{m+1}$. Applying the inverse of $\mathscr{A}(\vartheta^*,\boldsymbol{\zeta}^*)$ we arrive at

$$\left(I+\mathscr{A}(\vartheta^*,\boldsymbol{\zeta}^*)^{-1}\left(\mathscr{B}(\vartheta^*,\boldsymbol{\zeta}^*)\circ j+\mathscr{C}(\vartheta^*,\boldsymbol{\zeta}^*)\circ j_{\text{tr}}\right)\right)y=\mathscr{A}(\vartheta^*,\boldsymbol{\zeta}^*)^{-1}h \qquad \text{in } H^1_{\Gamma_D}(\Omega)^{m+1}.$$

Due to the compactness of j and j_{tr} we can apply Fredholm's theorem stating: for every $h\in(H^{-1}_{\Gamma_D})^m$, we will find a unique solution y to the above equation if the homogeneous equation admits only the trivial solution. Since $\mathscr{A}(\vartheta^*,\boldsymbol{\zeta}^*)$ is an isomorphism, we need to prove the uniqueness of solutions to the linearised equation (4.1). The *uniqueness for the linear part* follows by Proposition 5, with $\kappa(\vartheta)=\kappa(\vartheta^*)$, $\boldsymbol{a}=\kappa'(\vartheta^*)\nabla\vartheta^*$, and $\tilde{\boldsymbol{f}}(\cdot)\equiv 0$. The Fredholm theorem implies that the solution operator associated to the problem (4.1) $\mathscr{T}:(H^{-1}_{\Gamma_D})^{m+1}\to H^1_{\Gamma_D})^{m+1}$ is a linear continuous bijection.

Uniqueness: The uniqueness follows by Proposition 5, with $\kappa(\vartheta)=\kappa(\vartheta^*)$, $\boldsymbol{a}=\kappa'(\vartheta^*)\nabla\vartheta^*$, and

$$\boldsymbol{f}(\vartheta,\boldsymbol{\zeta})=\boldsymbol{f}'(\vartheta^*,\boldsymbol{\zeta}^*;\vartheta,\boldsymbol{\zeta})=D\boldsymbol{f}(\vartheta^*,\zeta^*)\begin{pmatrix}\vartheta\\ \zeta\end{pmatrix}=D\tilde{\boldsymbol{f}}(\boldsymbol{\zeta}_{\text{eq}}(\vartheta^*)-\zeta^*)\begin{pmatrix}\boldsymbol{\zeta}'_{\text{eq}}\vartheta\\ \zeta\end{pmatrix}.$$

Now let $\boldsymbol{y}\in(H^1_{\Gamma_D}(\Omega))^{m+1}$. Then $\mathscr{T}(y)+\boldsymbol{f}'(y_u;y)=:g\in(H^{-1}_{\Gamma_D}(\Omega))^{m+1}$ is an element in the dual space. For every element in the dual space, we find a solution to (4.1). The solution to the element $g\in(H^{-1}_{\Gamma_D}(\Omega))^{m+1}$ can due to the uniqueness only be y.

□

Theorem 10. *Let the assumptions of Theorem 9 be fulfilled. Then the control-to-state mapping $\mathscr{S}$: $W^{-1,p}_{\Gamma_D}(\Omega)\to W^{1,p}_{\Gamma_D}\times H^1(\Omega)^m$, $S(u)=y_u=(\vartheta_u,\boldsymbol{\zeta}_u)$, is directionally differentiable, and its directional derivative $y=\mathscr{S}'(Q;(w,\boldsymbol{r}))$ at $Q\in W^{-1,p}_{\Gamma_D}(\Omega)$ in the direction $(w,\boldsymbol{r})\in W^{-1,p}_{\Gamma_D}(\Omega)\times H^{-1}_{\Gamma_D}(\Omega)^m$ is given by the unique weak solution $y=(\vartheta,\boldsymbol{\zeta})\in(H^1_{\Gamma_D}(\Omega))^{m+1}$ of*

$$\left\{\begin{aligned}(\boldsymbol{v}\cdot\nabla)\vartheta-\Delta(\kappa(\vartheta_u)\vartheta)+\boldsymbol{L}\cdot\boldsymbol{f}'(\vartheta_u,\boldsymbol{\zeta}_u;\vartheta,\boldsymbol{\zeta})&= w && \text{in}\,\Omega\\ \boldsymbol{n}\cdot\nabla(\kappa(\vartheta_u)\vartheta)&= g'(\vartheta_u)\vartheta && \text{in}\,\Gamma_N,\quad \vartheta=0\quad \text{on}\,\Gamma_D\\ (\boldsymbol{v}\cdot\nabla)\boldsymbol{\zeta}-\boldsymbol{f}'(\vartheta_u,\boldsymbol{\zeta}_u;\vartheta,\boldsymbol{\zeta})&= \boldsymbol{r} && \text{in}\,\Omega,\quad \boldsymbol{\zeta}=0\quad \text{on}\,\Gamma_D,\end{aligned}\right. \tag{4.3}$$

where $\mathscr{S}(u)=y_u=(\vartheta_u,\boldsymbol{\zeta}_u)$,

Proof. We define $\mathscr{S}(u+\tau w)=y_\tau=(\vartheta_\tau,\boldsymbol{\zeta}_\tau)$. Then the functions $\bar{y}=1/\tau(y_\tau-y_u)-y$ fulfills the linearized state equation (4.2) with $\boldsymbol{f}\equiv 0$ and $(\vartheta^*,\boldsymbol{\zeta}^*)=(\vartheta_u,\boldsymbol{\zeta}_u)$ as well as the right-hand side $h\in W^{-1,p}_{\Gamma_D}(\Omega)\times H^{-1}_{\Gamma_D}(\Omega)^m$ given by

$$\begin{aligned}\langle h,(\varphi,\boldsymbol{\psi})\rangle=&\frac{1}{\tau}\int_\Omega(\kappa(\vartheta_u)-\kappa(\vartheta_\tau))(\nabla\vartheta_\tau-\nabla\vartheta_u)\cdot\nabla\varphi\,\mathrm{d}\boldsymbol{x}\\ &+\frac{1}{\tau}\int_\Omega\left(\kappa'(\vartheta_u)(\vartheta_\tau-\vartheta_u)-\kappa(\vartheta_\tau)+\kappa(\vartheta_u)\right)\cdot\nabla\varphi\,\mathrm{d}\boldsymbol{x}\\ &+\frac{1}{\tau}\int_\Omega(\rho\boldsymbol{L}\varphi-\boldsymbol{\psi})\left(\tau\boldsymbol{f}'(y_u,y)-(\boldsymbol{f}(y_\tau)-\boldsymbol{f}(y_u))\right)\mathrm{d}\boldsymbol{x}\\ &+\frac{1}{\tau}\int_{\Gamma_N}\left(g'(\vartheta_u)(\vartheta_\tau-\vartheta_u)-g(\vartheta_\tau)+g(\vartheta_u)\right)\varphi\,\mathrm{d}S.\end{aligned}$$

The directional differentiability of κ, $\boldsymbol{f}$, and g as well as the continuity of $\mathscr{S}$ (see Corollary 6 imply that the right-hand side vanishes as $\tau\to 0$. Since the left-had side of (4.2) defines a linear and bounded coercive operator on $H^1_{\Gamma_D}(\Omega)^{m+1}$, we may deduce that $\bar{y}=1/\tau(y_\tau-y_u)-y\to 0$ in $W^{1,p}_{\Gamma_D}\times H^1(\Omega)^m$ as $\tau\to 0$.

□

5 Optimal control problem

In the following, we focus on the optimal control of the state equations (2.6). Consider the cost functional

$$J(\vartheta,\boldsymbol{\zeta},u)=\frac{\alpha_1}{2}\int_{\Omega_1}[\vartheta_d-\vartheta]_+^2\,\mathrm{d}\boldsymbol{x}+\frac{\alpha_2}{2}\int_{\Omega_2}|\boldsymbol{\zeta}-\boldsymbol{\zeta}_d|^2\,\mathrm{d}\boldsymbol{x}+\frac{\alpha_3}{2}\int_{\Omega_3}u^2\,\mathrm{d}\boldsymbol{x}, \tag{5.1}$$

where $\vartheta_d\in L^2(\Omega)$, $\boldsymbol{\zeta}_d\in L^2(\Omega)^m$, $\Omega_i\subseteq\Omega$ and $\alpha_i>0$ for $i=1,2,3$. This is a standard tracking-type cost functional for the phase variable. Additionally the first part of the cost functional is needed in order to push the temperature into a reasonable regime in order to allow phase-changes.

Associated to the state equations (2.6), we introduce the control problem

$$\min\tilde{J}(u)=\min J(\vartheta_u,\boldsymbol{\zeta}_u,u)\,.$$

The functions ϑ_u and $\boldsymbol{\zeta}_u$ are the components of the solution to the state equation (2.6). First, we study the existence of a solution to the optimal control problem consisting of the functional (5.1) and the state equations (2.6).

Theorem 11. *Let the assumption 1 be fulfilled. Then there exists at least one optimal control to the functional* (5.1)*, where* $(\vartheta_u,\boldsymbol{\zeta}_u)$ *is the weak solution to* (2.6) *according to Definition 2.*

Proof. We prove the assertion via the standard direct approach in the calculus of variations. Let $\{u_n\}_{n\in\mathbb{N}}\subset L^2(\Omega)$ be a minimizing sequence to the functional, with associated solution $y_{u_n}=(\vartheta_{u_n},\boldsymbol{\zeta}_{u_n})$ to the system of state equations (2.6). Since (5.1) is bounded, we can extract a not-relabelled subsequence such that $u_n\rightharpoonup u$ weakly in L^2 such that $u_n\to u$ strongly in $W^{-1,p}$. From the continuity of the solution operator $\mathscr{S}$ to the system of state equations (2.6), we may infer that $y_{u_n}\to y$ in $W^{1,p}_{\Gamma_D}(\Omega)\times H^1_{\Gamma_D}(\Omega)^m$. The continuity of the functional u with respect to the convergence of $\vartheta_{u_n}\to\vartheta_u$ in $W^{1,p}_{\Gamma_D}(\Omega)$ and the weak-lower semi-continuity of the functional J (see (5.1)) with respect to weak convergence $u_n\rightharpoonup u$ in L^2 implies

$$J(\vartheta_u,\boldsymbol{\zeta}_u,u)\le\liminf_{n\to\infty}J(\vartheta_{u_n},\boldsymbol{\zeta}_{u_n},u_n)\le\lim_{n\to\infty}J(\vartheta_{u_n},\boldsymbol{\zeta}_{u_n},u_n)=\inf\,.$$

The infimum is attained since $\{u_n\}$ was assumed to be a minimizing sequence. □

Theorem 12. *Let the Assumptions 1 and 7 be fulfilled. If* $y_u=(\vartheta_u,\boldsymbol{\zeta}_u)$ *is a local optimum of* (5.1) *subjected to* (2.6)*, then it holds that*

$$\langle\tilde{J}'(u),w\rangle=\langle\partial_\vartheta J(\mathscr{S}(y_u),u),\mathscr{S}'(y_u;w)\rangle+\langle\partial_u J(\mathscr{S}(y_u),u),w\rangle\ge0\quad\textit{for all } w\in L^2(\Omega)\,. \tag{5.2}$$

Proof. Due to Theorem 10, the solution operator $\mathscr{S}:W^{-1,p}_{\Gamma_D}(\Omega)\times H^{-1}_{\Gamma_D}(\Omega)^m\to W^{1,p}_{\Gamma_D}(\Omega)\times H^1_{\Gamma_D}(\Omega)^m$ is directionally differentiable. Since $J:(W^{1,p}_{\Gamma_D}(\Omega)\times H^1_{\Gamma_D}(\Omega)^m)\times L^2(\Omega)\to\mathbb{R}$ is Fréchet differentiable, we infer the directional differentiability by [15, Lemma 3.9]. Note that $L^2(\Omega)\hookrightarrow^c W^{-1,p}_{\Gamma_D}(\Omega)$. □

Theorem 13 (Strong stationarity)**.** *Let the Assumptions 1 and 7 be fulfilled. If* u *with* $y_u=(\vartheta_u,\boldsymbol{\zeta}_u)$ *is a local optimum of* (5.1) *subjected to* (2.6)*, then there exists a* $(p,\boldsymbol{q})\in H^1_{\Gamma_D}(\Omega)^{d+1}$ *and a* $(\lambda_1,\boldsymbol{\lambda}_2)\in$

$L^2(\Omega)^{d+1}$ *such that*

$$\left\{\begin{array}{rcll} -(\boldsymbol{v}\cdot\nabla)p-\kappa(\vartheta_u)\Delta p+\lambda_1 &=& -\alpha_1\,[\vartheta_d-\vartheta_u]_+\Big|_{\Omega_1} & \text{in } \Omega\,,\\ \kappa(\vartheta_u)\boldsymbol{n}\cdot\nabla p+(\boldsymbol{v}\cdot\boldsymbol{n})p &=& g'(\vartheta_u)p & \text{on } \Gamma_N,\\ p &=& 0 & \text{on } \Gamma_D\,,\\ -(\boldsymbol{v}\cdot\nabla)\boldsymbol{q}-\varepsilon\Delta\boldsymbol{q}+\boldsymbol{\lambda}_2 &=& \alpha_2(\boldsymbol{\zeta}_u-\boldsymbol{\zeta}_d)\Big|_{\Omega_2} & \text{in } \Omega,\\ \varepsilon\boldsymbol{n}\cdot\nabla\boldsymbol{q}+(\boldsymbol{v}\cdot\boldsymbol{n})\boldsymbol{q} &=& \boldsymbol{0} & \text{on } \Gamma_N\,,\\ \boldsymbol{q} &=& \boldsymbol{0} & \text{on } \Gamma_D,\\ \alpha_3 u+\gamma p &=& 0 & \text{in } \Omega\,,\\ (\boldsymbol{L}\rho p-\boldsymbol{q})\boldsymbol{f}'((\vartheta_u,\boldsymbol{\zeta}_u);y) &\le& (\lambda_1(\boldsymbol{x}),\boldsymbol{\lambda}_2(\boldsymbol{x}))\cdot y & \text{for all } y\in\mathbb{R}^{m+1}\,. \end{array}\right. \tag{5.3}$$

Remark 14. *In the case that $y_u=(\vartheta_u,\boldsymbol{\zeta}_u)$ attains a value in the set, where $\boldsymbol{f}$ is continuously differentiable, we may write $\boldsymbol{f}'((\vartheta_u,\boldsymbol{\zeta}_u);y)=\partial_y\boldsymbol{f}(y_u)\cdot y=\partial_\vartheta\boldsymbol{f}(\vartheta_u,\boldsymbol{\zeta}_u)\vartheta+\partial_{\boldsymbol{\zeta}}\boldsymbol{f}(\vartheta_u,\boldsymbol{\zeta}_u)\cdot\boldsymbol{\zeta}$. Such that λ_1 and $\boldsymbol{\lambda}_2$ may be identified by*

$$\lambda_1=(L\rho p-\boldsymbol{q})\cdot\partial_\vartheta\boldsymbol{f}(\vartheta_u,\boldsymbol{\zeta}_u)\quad\text{and}\quad\boldsymbol{\lambda}_2=(L\rho p-\boldsymbol{q})\cdot\partial_{\boldsymbol{\zeta}}\boldsymbol{f}(\vartheta_u,\boldsymbol{\zeta}_u)\,.$$

In comparisson with the assumption 1, we note that functions in $W^{1,\infty}([a,b];\mathbb{R})$ are a.e. Lipschitz functions and thus of bounded variation. Functions of bounded variation are known to be differentiable a.e. [16]. But note that this holds for a.e. $(\vartheta_u,\boldsymbol{\zeta}_u)\in\mathbb{R}^{m+1}$ and thus not for a.e. $\boldsymbol{x}\in\Omega$.

Proof. An approximation argument, by approximating the function $\boldsymbol{f}$ by $\mathscr{C}^1$-functions $\boldsymbol{f}_\varepsilon$ and passing to the limit with the regularization grants all but the last of the above relations. Indeed, since for the case $\varepsilon>$, the above relation holds with $(\lambda_1,\boldsymbol{\lambda}_2)=\boldsymbol{f}'(\vartheta_u,\boldsymbol{\zeta}_u)$ since the associated solution operator is Fréchet differentiable by standard theory. Passing to the limit with $\varepsilon\to0$ we infer (5.3) without the inequality relation. The associated *a priori* estimates can be deduced by Theorem 3 and 10. We refer to [17] for such an approach.

The last relation follows from Theorem 12 and the density of the solution operator associated to the linearized equation (see Theorem 9 and compare to [18]). Indeed, let $y=\mathscr{S}'(y_u;(\gamma w,\boldsymbol{0}))$, then we may test (4.1) with $(w,\boldsymbol{r})=(\gamma w,\boldsymbol{0})$ by $p,\boldsymbol{q}$ in order to infer

$$\begin{aligned}-\int_\Omega((\boldsymbol{v}\cdot\nabla)p+\Delta p\kappa(\vartheta_u))\vartheta+((\boldsymbol{v}\cdot\nabla)\boldsymbol{q}+\varepsilon\Delta\boldsymbol{q})\cdot\boldsymbol{\zeta}\,\mathrm{d}\boldsymbol{x}&\\ +\int_{\Gamma_N}g'(\vartheta_u)p\vartheta\,\mathrm{d}S+\int_\Omega(\boldsymbol{L}\rho p-\boldsymbol{q})\boldsymbol{f}'(y_u;y)\,\mathrm{d}\boldsymbol{x}&=\int_\Omega\gamma wp\,\mathrm{d}\boldsymbol{x}.\end{aligned}$$

By inserting the first seven relations of (5.3), we infer that

$$\begin{aligned}&\int_\Omega(\boldsymbol{L}\rho p-\boldsymbol{q})\boldsymbol{f}'(y_u;y)-\lambda_1\vartheta-\boldsymbol{\lambda}_2\cdot\boldsymbol{\zeta}\,\mathrm{d}\boldsymbol{x}\\ &\qquad=\int_{\Omega_1}\alpha_1\,[\vartheta_d-\vartheta_u]_+\,\vartheta\,\mathrm{d}\boldsymbol{x}-\int_{\Omega_2}\alpha_2(\boldsymbol{\zeta}_u-\boldsymbol{\zeta}_d)\cdot\boldsymbol{\zeta}\,\mathrm{d}\boldsymbol{x}-\int_{\Omega_3}\alpha_3uw\,\mathrm{d}\boldsymbol{x}.\end{aligned}$$

From the Theorem 12, we derive by calculating the expressions explicitly that

$$\begin{aligned}0&\le\langle\partial_\vartheta J(\mathscr{S}(y_u),u),\mathscr{S}'(y_u;w)\rangle+\langle\partial_u J(\mathscr{S}(y_u),u),w\rangle\\ &=-\int_{\Omega_1}\alpha_1\,[\vartheta_d-\vartheta_u]_+\,\vartheta\,\mathrm{d}\boldsymbol{x}+\int_{\Omega_2}\alpha_2(\boldsymbol{\zeta}_u-\boldsymbol{\zeta}_d)\cdot\boldsymbol{\zeta}\,\mathrm{d}\boldsymbol{x}+\int_{\Omega_3}\alpha_3uw\,\mathrm{d}\boldsymbol{x},\end{aligned}$$

which implies that

$$\int_\Omega (\boldsymbol{L}\rho p - \boldsymbol{q})\boldsymbol{f}'(y_u;y) - (\lambda_1, \boldsymbol{\lambda}_2)\cdot y \,\mathrm{d}\boldsymbol{x} \le 0 \quad \text{for all } w \in L^2(\Omega) \text{ such that } y = \mathscr{S}'(y_u;w)\,.$$

The range of the operator $\mathscr{S}'(y_u;\cdot)$ is dense in $(H^1_{\Gamma_D})^{m+1}$ such that we infer that

$$\int_\Omega (\boldsymbol{L}\rho p - \boldsymbol{q})\boldsymbol{f}'(y_u;y) - (\lambda_1, \boldsymbol{\lambda}_2)\cdot y \,\mathrm{d}\boldsymbol{x} \le 0 \quad \text{for all } y \in L^2(\Omega)^{m+1}\,,$$

where we used that $H^1_{\Gamma_D}(\Omega)$ is dense in $L^2(\Omega)$. Since all appearing terms are integrable, the assertion also holds a.e. in Ω and for all directions, *i.e.*,

$$(\boldsymbol{L}\rho p - \boldsymbol{q})\boldsymbol{f}'(y_u;y) - (\lambda_1, \boldsymbol{\lambda}_2)\cdot y \le 0 \quad \text{for all } y \in \mathbb{R}^{m+1}\,.$$

□

6 Numerical results

In this section we present some preliminary numerical results for the optimal control of laser beam shaping. To simplify the exposition, we consider $\boldsymbol{\zeta}$, the vector containing the steel phases to be unidimensional, ζ, as it will only contain the volume fraction of liquid steel. Equivalently, the vector $\boldsymbol{L}$ will contain only latent heat for the melting process, L. To avoid transformation of material data, we consider the system (2.5) before the enthalpy transformation. As the computational domain we consider a rectangular plate, where the upper surface, to be impinged by the laser beam is in the plane $\{z=0\}$. The bottom face on which we assume the homogeneous Dirichlet condition is in the plane $\{z=-z_{max}\}$.

Using the cost functional $J(\theta,\zeta,u)$ from (5.1) and assuming that $\tilde{\boldsymbol{f}}$ is continuously differentiable, the resultant adjoint system with variables p and q equivalent to (5.3) is

$$\left\{\begin{array}{rcll}
-\tilde{\eta}\,(\theta)\,(\boldsymbol{v}\cdot\nabla)p - \tilde{\kappa}(\theta)\Delta p + \rho\boldsymbol{L}\cdot\tilde{\boldsymbol{f}}_\vartheta(\theta,\boldsymbol{\zeta}_u)p & & & \\
+\tilde{\boldsymbol{f}}_\vartheta(\vartheta_u,\boldsymbol{\zeta}_u)\cdot\boldsymbol{q} & = & -\alpha_1\,[\vartheta_d-\theta]_+\Big|_{\Omega_1} & \text{in } \Omega, \\
\tilde{\kappa}(\theta)\boldsymbol{n}\cdot\nabla p + \tilde{\eta}\,(\theta)\,(\boldsymbol{v}\cdot\boldsymbol{n})p & = & hp & \text{on } \Gamma_N, \\
p & = & 0 & \text{on } \Gamma_D, \\
-(\boldsymbol{v}\cdot\nabla)\boldsymbol{q} - \varepsilon\Delta\boldsymbol{q} - \tilde{\boldsymbol{f}}_{\boldsymbol{\zeta}}(\theta,\boldsymbol{\zeta}_u)\cdot\boldsymbol{q} + \rho\boldsymbol{L}\cdot\tilde{\boldsymbol{f}}_{\boldsymbol{\zeta}}(\theta,\boldsymbol{\zeta}_u)p & = & \alpha_2(\boldsymbol{\zeta}_u-\boldsymbol{\zeta}_d)\Big|_{\Omega_2} & \text{in } \Omega, \\
\varepsilon\boldsymbol{n}\cdot\nabla\boldsymbol{q} + (\boldsymbol{v}\cdot\boldsymbol{n})\boldsymbol{q} & = & \boldsymbol{0} & \text{on } \Gamma_N, \\
\boldsymbol{q} & = & \boldsymbol{0} & \text{on } \Gamma_D,
\end{array}\right. \tag{6.1}$$

In order to build a reasonable numerical finite element scheme only relying on $P1$ finite elements, an auxiliary variable $\omega = \tilde{\kappa}(\theta)\Delta p$ is added equipped with appropriate boundary conditions.

We chose the control term Q, i.e., the power absorbed by the plate, on the right-hand side of (2.1) to be of the form $Q = u\gamma$, where u will act as the control in our optimal control problem. To realize a realistic solid state laser power distribution, γ is introduced as a projection factor. We choose γ according to a simplified power distribution model restricting the absorbed power. It has a super-Gaussian profile [19] in the laser feed direction and has an exponential decay in the depth of the plate. On the other hand, there is no restriction on the laser profile in the transverse direction of movement, which is then main goal of our design task.

This way γ is defined as

$$\gamma(\boldsymbol{x}) = \gamma_1(x)\chi_{[0,\bar{y}]}(y)\exp(c_3 z) \quad \text{with} \quad \gamma_1(x) = 1 - \left(1 - \exp\left(\frac{-x^2}{(\bar{x}/2)^2}\right)\right)^{c_1}, \tag{6.2}$$

where $\gamma_1(x)$ represents a super-Gaussian profile which is common in solid state laser modelling [19, 20, 21].

This profile is also known as flat-top profile. The expression used in (6.2) was extracted from [22].

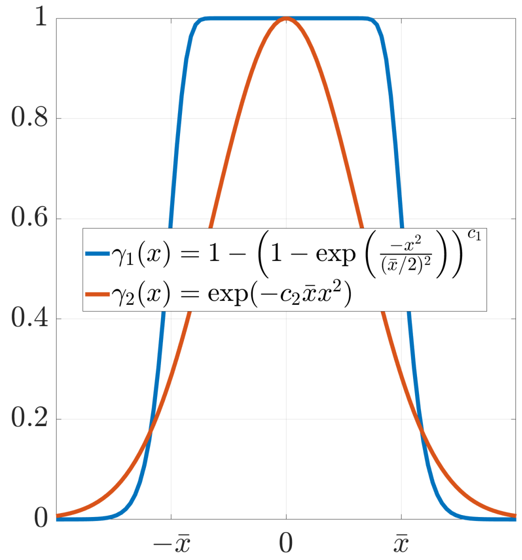

Figure 1: Comparison of super-Gaussian (γ_1) and Gaussian (γ_2) profiles.

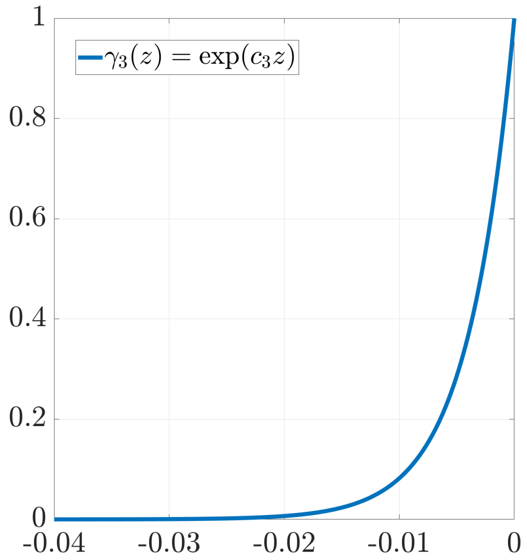

Figure 2: Exponential decay from surface to bottom of a plate.

The super-Gaussian profile is defined by the parameter $\bar{x}$, related to the length of the laser, and the constant c_1, which adjusts the flatness. Among the other terms in γ we find the function $\chi_{[-\bar{y},\bar{y}]}(y)$ which is the characteristic function of the interval which defines the maximal width of the laser beam orthogonally to the laser feed direction. For numerical efficiency, only half the domain will be used for numerical simulations with a symmetry boundary condition on the plane $\{y = 0\}$. Finally, to account for the fact that most of the power power is absorbed in the vicinity of the surface is modeled by an exponential decay in the z-direction.

We apply a standard gradient descent to solve the optimal control problem numerically. To this end we have to iterate solving the state system (2.5) and the adjoint system (6.1) and update the control based on a linesearch in the negative gradient direction, see (5.3.7) until a convergence condition is fulfilled.

We utilize the Finite Element Method (FEM) using the finite element package *pdelib2* [23] developed and maintained at WIAS. The nonlinearities together with the coupling of (2.5a)-(2.5c) were solved using a fixed-point algorithm and an adaptive mesh module was used to refine the mesh based on a residual-based a posteriori error estimator determining regions with steep gradients for the temperature and melting fraction [24]. Note that the phase transition equation (2.3) cannot be solved directly using FEM without encountering erroneous results and thus we use the Streamline-Upwind Petrov-Galerkin (SUPG) stabilization method to achieve a correct solution [25, 26]. This mesh is reused for the adjoint system (6.1) which can be solved instead in one single step. The algorithm is completed with a simple gradient step in order to infer the updated control, which is the laser power.

As data for the numerical approximation, we consider a $40\,\mathrm{mm}$ thick Raex® 400 steel plate moving with a speed of $135\,\mathrm{mm/min}$. The typical melting profile (melting pool) created by a laser acting on the top plain surface of a plate often has the shape of an eyelid [27, 28, 29]. By minimizing the cost functional J from (5.1), we aim to find find a laser power distribution u that achieves a liquid trail ζ close to a rectangular ($5 \times 2.5\,\mathrm{mm}^2$) shape, which thus defines ζ_d. The first term $[\theta_d - \theta]_+^2$ in (5.1)with θ_d being close to the melting temperature (1517 ℃) has been introduced in order to steer the system in reach of creating a liquid trail, even if the initial power may not cause melting, *e.g.*, $u \equiv 0$,

The steel properties required for the model are the density, specific heat and thermal conductivity. They were derived using the commercial software JMatPro® [30]. This software mainly requires as input the chemical composition of the steel, which we chose according to Raex® 400. Regarding the phase equation (2.3), the function $\tilde{f}(\theta,\zeta)$ is defined in (2.4) as

$$\tilde{f}(\theta,\zeta) = \frac{1}{\tau_\zeta}[\zeta_{eq}(\theta) - \zeta]_+ \tag{6.3}$$

Here, $\zeta_{eq}(\theta)$ represent the equilibrium volume fraction of liquid at temperature θ.

It should have the maximum value 1, when the temperature exceeds 1537 ℃ (melting point). We define $\zeta_{eq}(\theta) = H_{\delta_1}(\theta - 1537 + \delta_1)$, where H_{δ_1} is a regularization of the Heaviside function. The value of τ_ζ representing the transformation velocity is $10^{-2}\,\mathrm{s}$. Furthermore, the latent heat value for the melting reaction is $272\,\mathrm{kJ/kg}$. This choice for $\zeta_{eq}(\theta)$ complies with the assumptions in Section 3.

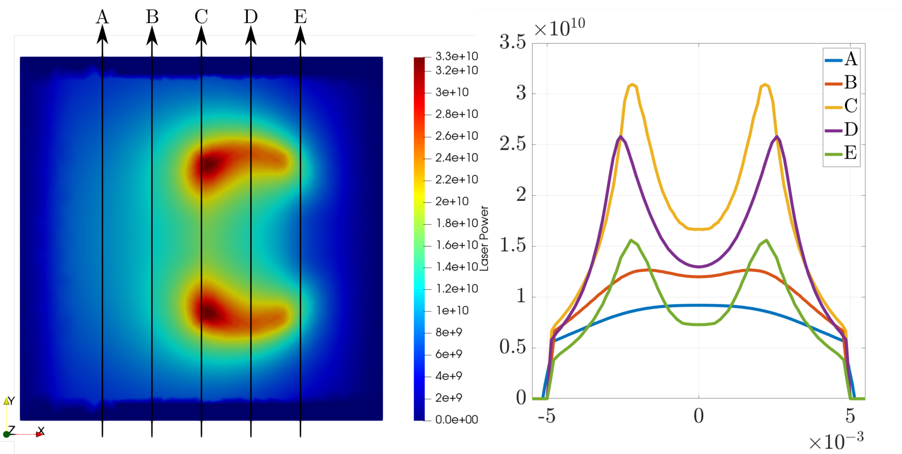

Figure 3: Optimal control $u\gamma$.

In Figure 3 we show the top view of the laser power in the subdomain Ω_1 for the case of the desired rectangular cross section of the liquid trail. The view is reflected from the symmetry plane for a better comprehension. Moreover, due to non-uniform distribution of the power, a set of lines A to E are used to plot cross sections of the laser power in the y-direction. As expected, to realize a more rectangular cross section of the liquid trail a bi-modal power distribution with maxima close to the boundary of the desired liquid profile is required.

Figure 4 displays several iterations of the control on the plate surface in the cross section of the liquid profile along the C-line (see Figure 3). It can be seen how the power profile gradually moves from an initial Gaussian shape to one with a flattened top and then to the optimal bi-modal shape.

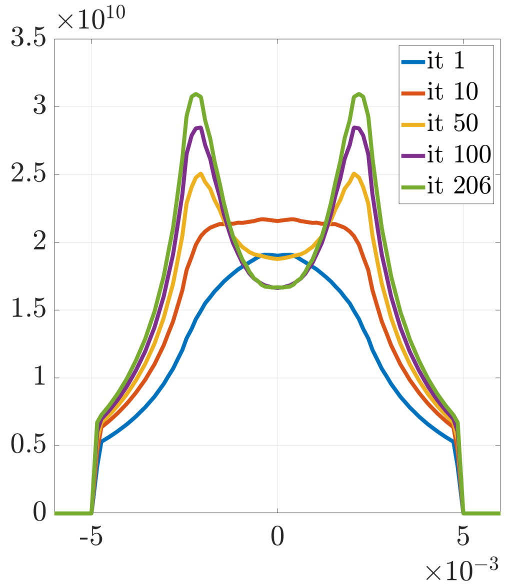

Figure 4: Evolution of the restricted control $\bar{u}$ along the y-axis (C-line, see Figure 3).

In order to shed some light on the improvement achieved by the algorithm, in Figure 5 we compare the heat distribution of an early iterate with the heat distribution of the optimal one. The initial power distribution was overheating the steel in the centre of the desired liquid trail but afterwards with the optimized power distribution, the heat distribution is broadened and more homogeneous in the optimized state.

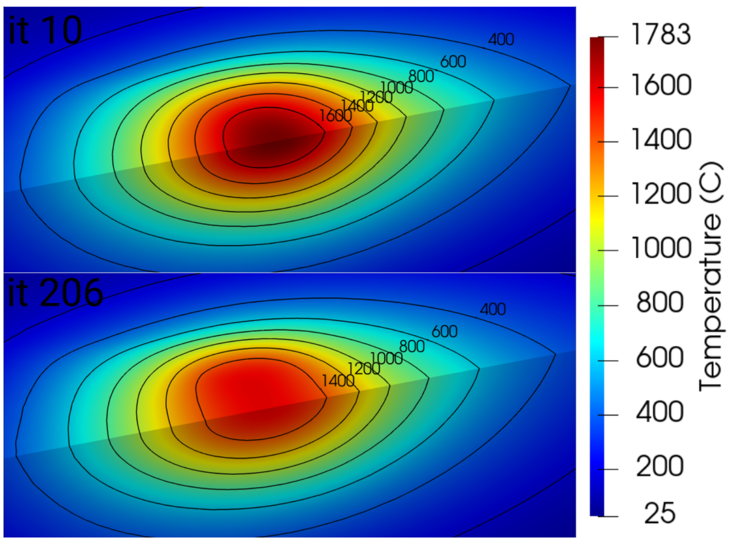

Figure 5: Comparison of temperature distribution, for initial Gaussian power (top) and optimal bimodal intensity distribution (bottom).

Finally, to illustrate the effect of velocity, Figure 6 depicts the resulting temperature distributions for growing velocity. More precisely, the temperature field obtained by the optimal control for velocities 135, 270 and 675 mm/min is represented. As expected it shows a growing dissipation of temperature against the direction of the movement with increasing speed.

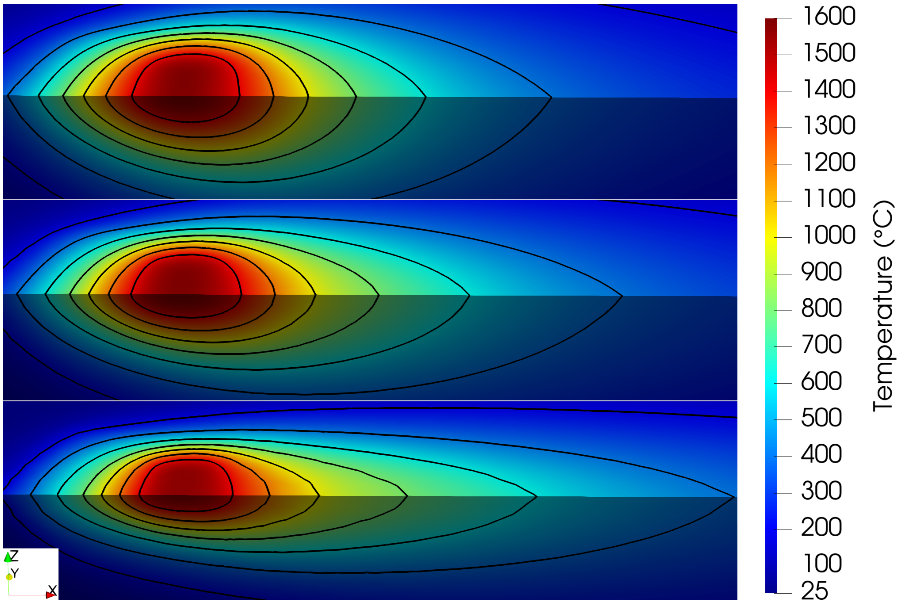

Figure 6: Comparison of temperature generated by the optimal control in three cases with different velocity. From top to bottom: 135, 270 and 675 mm/min.

7 Conclusions

We have investigated the laser beam shaping problem in terms of an optimal control problem for a material that can undergo phase changes during heating. The system of PDEs has been analysed to prove the existence, uniqueness and regularity of solutions and a strong stationarity result for the optimal control problem. The optimal control problem was solved numerically applying FEM and the projected gradient method [31] to achieve a desired melting profile. The package *pdelib2* [23] was used for this purpose.

These first numerical results show indeed that the suggested optimal control approach can offer a viable solution for many beam shaping applications including Selective Laser Melting (SLM) processes in 3D metal printing. However, in this case a more involved model including different printed layers and the different steel phases appearing due to melting and remelting should be considered.

From an analytical point of view, the derivation of second order sufficient conditions would be a challenging task. But this is especially impeded by the low regularity of the nonlinear couplings of the equations due to the function f and would require additional care in deriving optimality conditions.

References

[1] M. Traub, *Beam Shaping for Laser Material Processing*. Springer International Publishing, 2024, pp. 239–244. Available: https://doi.org/10.1007/978-3-030-98323-9_3

[2] S. A. Khairallah, A. T. Anderson, A. Rubenchik, and W. E. King, “Laser powder-bed fusion additive manufacturing: Physics of complex melt flow and formation mechanisms of pores, spatter, and denudation zones,” *Acta Materialia*, vol. 108, pp. 36–45, 2016.

[3] J. Bi, L. Wu, S. Li, Z. Yang, X. Jia, M. D. Starostenkov, and G. Dong, “Beam shaping technology

and its application in metal laser additive manufacturing: A review," *Journal of Materials Research and Technology*, vol. 26, pp. 4606–4628, 2023.

[4] T. M. Wischeropp, H. Tarhini, and C. Emmelmann, "Influence of laser beam profile on the selective laser melting process of AlSi10Mg," *Journal of Laser Applications*, vol. 32, no. 2, p. 022059, 05 2020.

[5] D. Hömberg and W. Weiss, "PID control of laser surface hardening of steel," *IEEE Transactions on Control Systems Technology*, vol. 14, no. 5, pp. 896–904, Sep. 2006.

[6] E. Casas and F. Tröltzsch, "First- and second-order optimality conditions for a class of optimal control problems with quasilinear elliptic equations," *SIAM Journal on Control and Optimization*, vol. 48, no. 2, pp. 688–718, 2009.

[7] P. Druet, O. Klein, J. Sprekels, F. Tröltzsch, and I. Yousept, "Optimal control of three-dimensional state-constrained induction heating problems with nonlocal radiation effects," *SIAM Journal on Control and Optimization*, vol. 49, no. 4, pp. 1707–1736, 2011.

[8] E. Casas, "Boundary control problems for quasi-linear elliptic equations: A pontryagin's principle," *Applied Mathematics and Optimization*, vol. 33, no. 3, pp. 265–291, 1996.

[9] M. Křížek and L. Liu, "On the maximum and comparison principles for a steady-state nonlinear heat conduction problem," *ZAMM - Journal of Applied Mathematics and Mechanics / Zeitschrift für Angewandte Mathematik und Mechanik*, vol. 83, no. 8, pp. 559–563, 2003.

[10] D. Rosenthal, "Mathematical theory of heat distribution during welding and cutting," *Welding journal*, vol. 20, pp. 220–234, 1941.

[11] J. Nečas, *Les Méthodes Directes En Théorie Des Équations Elliptiques*. Masson, Paris., 1967.

[12] F. Demengel and G. Demengel, *Functional Spaces for the Theory of Elliptic Partial Differential Equations*. London: Springer, 2012.

[13] T. Roubíček, *Nonlinear partial differential equations with applications*. Birkhäuser, Basel, 2005. Available: https://www.google.com/books/edition/_/lgElHFuIDLUC

[14] R. Haller-Dintelmann, C. Meyer, J. Rehberg, and A. Schiela, "Hölder continuity and optimal control for nonsmooth elliptic problems," *Appl. Math. Optim.*, vol. 60, no. 3, pp. 397–428, Dec. 2009.

[15] R. Herzog, C. Meyer, and G. Wachsmuth, "B- and strong stationarity for optimal control of static plasticity with hardening," *SIAM Journal on Optimization*, vol. 23, no. 1, pp. 321–352, 2013.

[16] I. P. Natanson, *Theorie der Funktionen einer reellen Veränderlichen*, ser. Übersetzung aus dem Russischen. Dritte Auflage. Herausgegeben von Karl Bögel. Mathematische Lehrbücher und Monographien. Abteilung I: Mathematische Lehrbücher, Band VI. Akademie-Verlag, Berlin, 1969.

[17] A. R. Christian Clason, Vu Huu Nhu, "Optimal control of a non-smooth quasilinear elliptic equation," *Mathematical Control & Related Fields*, vol. 11, no. 3, pp. 521–554, 2021.

[18] L. M. Betz, "Strong stationarity for optimal control of a nonsmooth coupled system: Application to a viscous evolutionary variational inequality coupled with an elliptic pde," *SIAM Journal on Optimization*, vol. 29, no. 4, pp. 3069–3099, 2019.

[19] S. De Silvestri, P. Laporta, V. Magni, and O. Svelto, “Solid-state laser unstable resonators with tapered reflectivity mirrors: the super-gaussian approach,” *IEEE journal of quantum electronics*, vol. 24, no. 6, pp. 1172–1177, 1988.

[20] X. Liu, Y. Zhao, A. Yang, and W. Xie, “Super-gaussian pumping profiles for solid state lasers,” in *Solid State Lasers XVI: Technology and Devices*, vol. 6451. International Society for Optics and Photonics, 2007, p. 645120.

[21] V. Prakapenka, A. Kubo, A. Kuznetsov, A. Laskin, O. Shkurikhin, P. Dera, M. Rivers, and S. Sutton, “Advanced flat top laser heating system for high pressure research at gsecars: application to the melting behavior of germanium,” *High Pressure Research*, vol. 28, no. 3, pp. 225–235, 2008.

[22] Y. Li, “Flat-topped light beams with non-circular cross-sections,” *Journal of modern optics*, vol. 50, no. 13, pp. 1957–1966, 2003.

[23] Weierstrass Institute (WIAS), “pdelib2.” Available: https://www.wias-berlin.de/software/pdelib/.” [Accessed on: 11 Dec 2020]

[24] D. Hömberg, Q. Liu, J. Montalvo-Urquizo, D. Nadolski, T. Petzold, A. Schmidt, and A. Schulz, “Simulation of multi-frequency-induction-hardening including phase transitions and mechanical effects,” *Finite Elements in Analysis and Design*, vol. 121, pp. 86–100, Nov. 2016.

[25] M. Augustin, A. Caiazzo, A. Fiebach, J. Fuhrmann, V. John, A. Linke, and R. Umla, “An assessment of discretizations for convection-dominated convection–diffusion equations,” *Computer Methods in Applied Mechanics and Engineering*, vol. 200, no. 47-48, pp. 3395–3409, Nov. 2011.

[26] M. J. Arenas, D. Hömberg, R. Lasarzik, P. Mikkonen, and T. Petzold, “Modelling and simulation of flame cutting for steel plates with solid phases and melting,” *Journal of Mathematics in Industry*, vol. 10, no. 18, Jun. 2020.

[27] S. Ghosh, L. Ma, L. E. Levine, R. E. Ricker, M. R. Stoudt, J. C. Heigel, and J. E. Guyer, “Single-track melt-pool measurements and microstructures in inconel 625,” *JOM*, vol. 70, no. 6, pp. 1011–1016, feb 2018.

[28] E. Soylemez, “Modeling the melt pool of the laser sintered Ti6Al4V layers with Goldak’s double-ellipsoidal heat source,” 2018.

[29] S. Kollmannsberger, M. Carraturo, A. Reali, and F. Auricchio, “Accurate prediction of melt pool shapes in laser powder bed fusion by the non-linear temperature equation including phase changes,” *Integrating Materials and Manufacturing Innovation*, vol. 8, no. 2, pp. 167–177, apr 2019.

[30] N. Saunders, U. K. Z. Guo, X. Li, A. P. Miodownik, and J. P. Schillé, “Using JMatPro to model materials properties and behavior,” *JOM*, vol. 55, no. 12, pp. 60–65, Dec. 2003.

[31] F. Tröltzsch, *Optimal control of partial differential equations: theory, methods, and applications*. American Mathematical Soc., 2010, vol. 112.